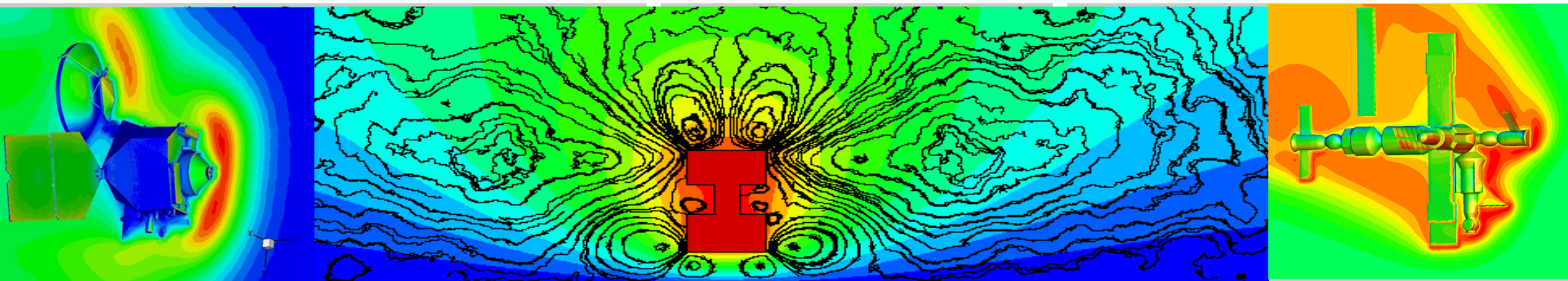


Exceptional service in the national interest



Molecular-Level Simulations of Non-equilibrium Flows in Gases

Michael A. Gallis

Engineering Sciences Center
Sandia National Laboratories
Albuquerque, New Mexico, USA

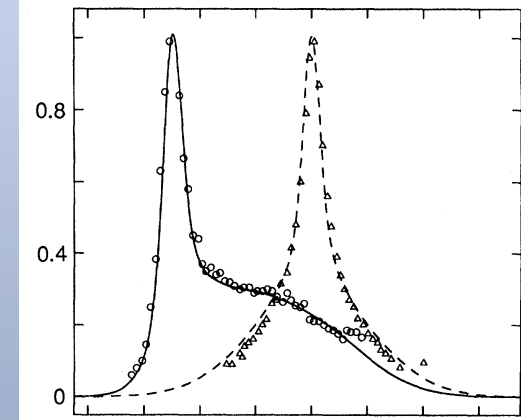


Sandia National Laboratories is a multi-program laboratory managed and operated by Sandia Corporation, a wholly owned subsidiary of Lockheed Martin Corporation, for the U.S. Department of Energy's National Nuclear Security Administration under contract DE-AC04-94AL85000.

Non-equilibrium effects

Non-equilibrium effects:

- Non-Maxwell, Chapman-Enskog velocity distribution functions
- Non-linear transport properties
- Non-Boltzmann internal energy, no energy equipartition
- Non-Arrhenius chemical reactions
- Non-continuous temperature and velocity profiles (Knudsen layers close to walls)



Non-equilibrium velocity distribution functions in the front a Mach 25 normal shock of helium
Pham-Van-Diep, *et al.*, *Science*, 1989

- Can be caused by:
 - Reduced collisionality (low density)
 - Strong gradients even in near-continuum conditions

Boltzmann Equation and the Direct Simulation Monte Carlo Method (DSMC)



Ludwig
Boltzmann

$$\frac{\partial f}{\partial t} + \mathbf{v} \cdot \frac{\partial f}{\partial \mathbf{x}} + \frac{\mathbf{F}}{m} \cdot \frac{\partial f}{\partial \mathbf{v}} = \int_{-\infty}^{\infty} \int_0^{4\pi} (f^* f_1^* - f f_1) |\mathbf{v} - \mathbf{v}_1| \sigma d\Omega d\mathbf{v}_1$$

molecular motion and
force-induced acceleration

pairwise molecular collisions
(molecular chaos)



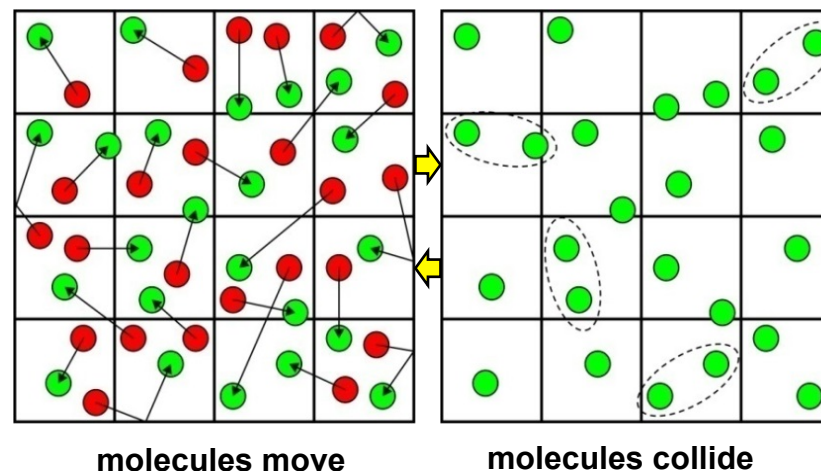
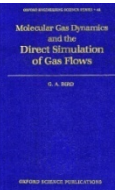
James Clerk
Maxwell

$f(\mathbf{r}, \mathbf{c}, t) d^3 r d^3 c \rightarrow$ Expected number of molecules at time t in at $\mathbf{r} + d^3 r, \mathbf{c} + d^3 c$

$$n(\mathbf{r}, t) = \int f(\mathbf{r}, \mathbf{c}, t) d^3 c$$



Graeme Bird
(1963, 1994)



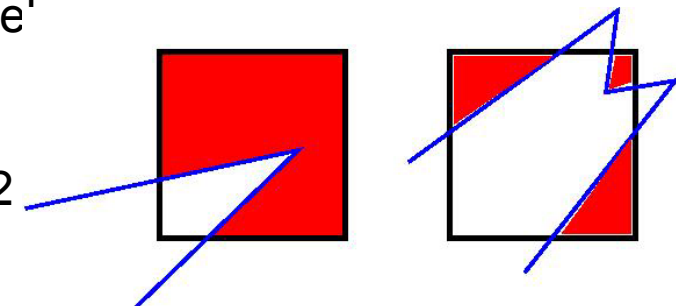
DSMC is a **physical, statistical, molecular-level** simulation method

Developing an Exascale DSMC Code

SPARTA = Stochastic PArallel Rarefied-gas Time-accurate Analyzer

General features

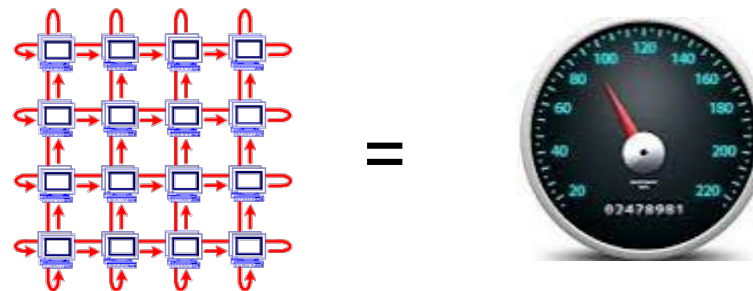
- 1D, 2D, 2D-axisymmetric or 3D, serial or parallel
- Cartesian, hierarchical grid
 - Oct-tree (up to 16 levels in 64-bit cell ID)
 - Multilevel, general $N \times M \times L$ instead of $2 \times 2 \times 2$
- Triangulated surfaces cut/split the grid cells
 - 3D via Schwartzentruber algorithm
 - 2D via Weiler/Atherton algorithm
 - Formulated so can use as kernel in 3D algorithm
- C++, but really object-oriented C
 - Designed to be easy to extend
 - New collision/chemistry models, boundary conditions, etc.
- Code available at <http://sparta.sandia.gov>



Parallel Efficiency: The Unfair Advantage

- The advantages of DSMC come at a cost
- DSMC is **computationally efficient** but **computationally intense**
- Its successful application to real problems depends heavily on its parallel performance
- **1000x speedup** required for some problems of interest
- Monte Carlo methods usually have good parallel performance
 - The workload depends mainly on the molecules within a cell
 - Relatively less need to communicate information between cells
 - Trivial to parallelize in velocity space

The necessary speedup can be achieved without any loss of accuracy or convergence characteristics through parallel computing



Top 5 Supercomputers (2014)

Rank	Site	System	Cores	Rmax (TFlop/s)	Rpeak (TFlop/s)
1	National Super Computer Center in Guangzhou	Tianhe-2 (MilkyWay-2) - TH-IVB-FEP Cluster, Intel Xeon E5-2692 12C 2.200GHz, TH Express-2, Intel Xeon Phi 31S1P	3,120,000	33,862.7	54,902.4
2	DOE/SC/Oak Ridge National Laboratory	Titan - Cray XK7 , Opteron 6274 16C 2.200GHz, Cray Gemini interconnect, NVIDIA K20x	560,640	17,590.0	27,112.5
3	DOE/NNSA/LLNL	Sequoia - BlueGene/Q, Power BQC 16C 1.60 GHz, Custom	1,572,864	17,173.2	20,132.7
4	RIKEN Advanced Institute for Computational Science (AICS)	K computer , SPARC64 VIIIfx 2.0GHz, Tofu interconnect	705,024	10,510.0	11,280.4
5	DOE/SC/Argonne National Laboratory	Mira - BlueGene/Q, Power BQC 16C 1.60GHz, Custom	786,432	8,586.6	10,066.3

24h hr run on Sequoia = 4,310 years CPU time

Programming for Next Generation and Exascale Machines

Goal is to decouple the science code from the hardware details

Envisaged Next Generation Platforms:

- Millions of nodes likely
- Reduced memory per node
- Parallelism within node:
 - Multi-core: 16 and growing
 - Many-core: Intel Xeon Phi, 240 threads
 - GPUs: NVIDIA/AMD, 1000 warps
- **Example:** LLNL BG/Q: 96K nodes, 16 cores/node + 4 MPI tasks/core

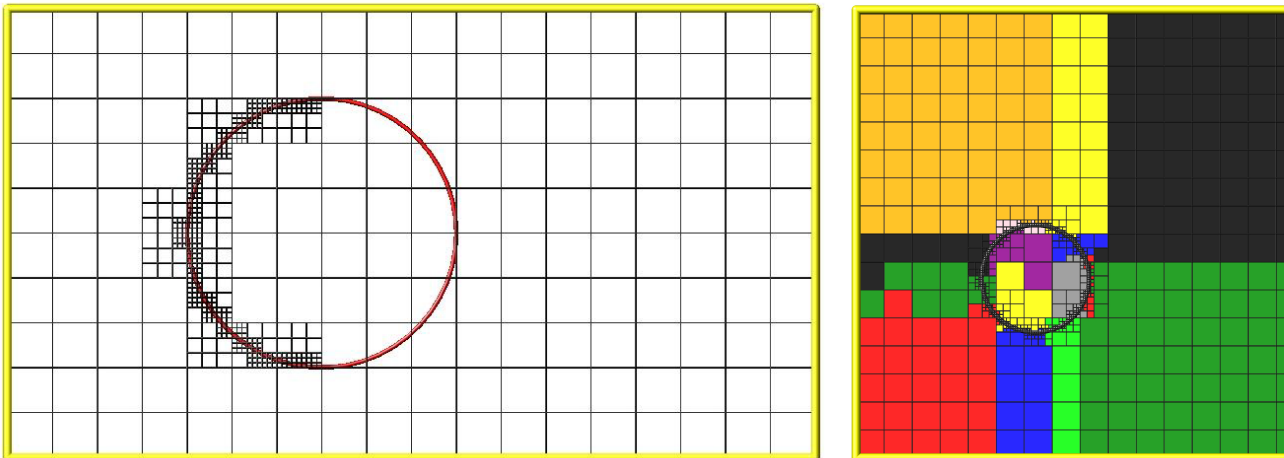
Necessary elements

- Adaptive gridding
- In-situ visualization
- Efficient communications
- Load balancing



Adaptive Gridding

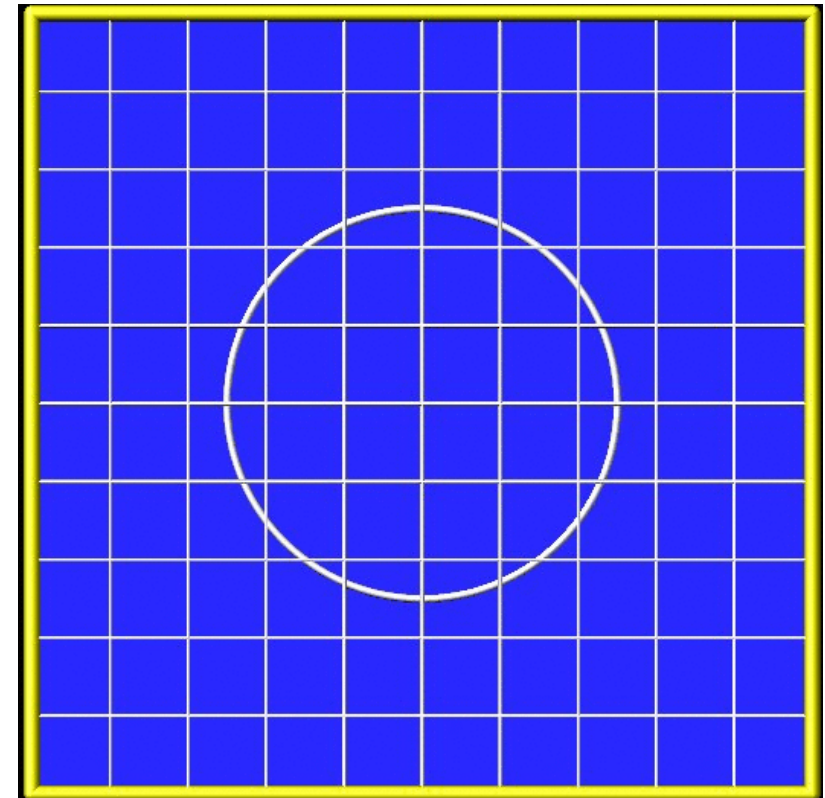
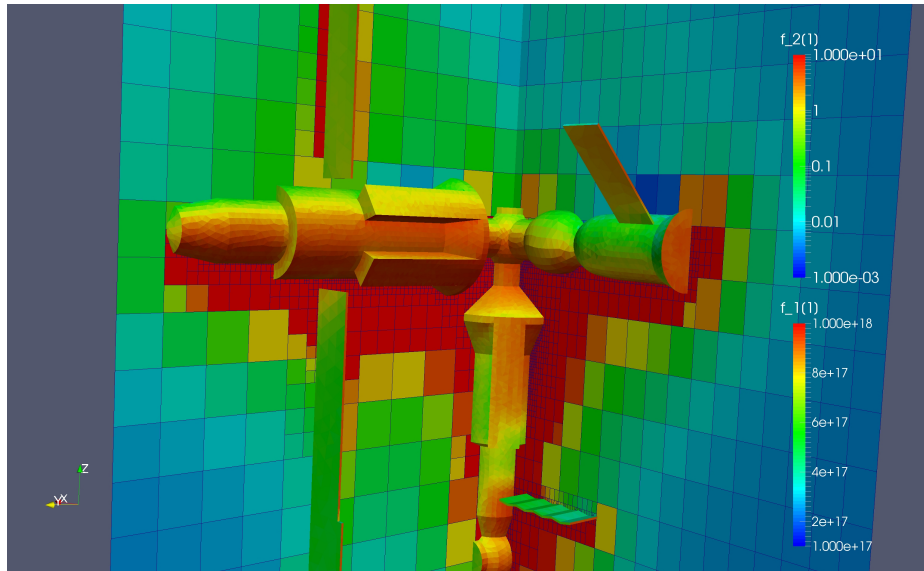
- **Create/adapt grid in situ, rather than pre-process & read in**
- Examples: Generate around surface to user-specified resolution, adapt grid based on flow properties
- Algorithms should be efficient if they require only **local communications**



- Another setup task: label cells as outside/inside
- Simple if pre-processing, in situ easier for large problems

Adaptive Gridding

Mir space station with 5-levels of adaptive grid

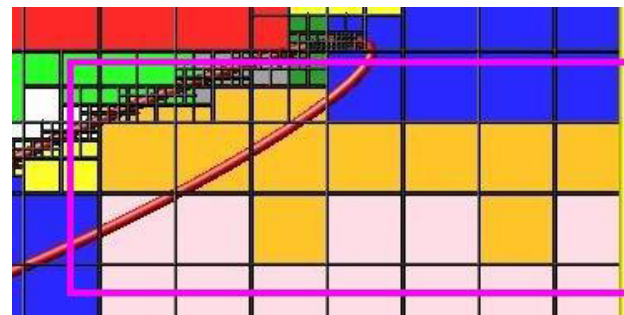
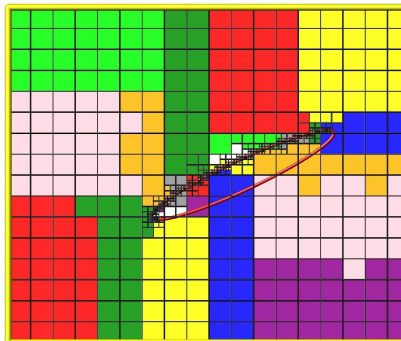


Example of multiple-level grid generation in 2D

Efficient Communication & Load Balancing

To achieve maximum efficiency:

- One communication per step
 - Multiple passes if needed (or can bound molecule move)
- Communication with modest count of neighbor processors
- One processor = compact clump of cells via load balancing
 - Ghost region = nearby cells within user-defined cutoff
 - Store surface information for ghost cells to complete move



Example:
 1B cells on 1024 BG/Q node
 Worst case: move all cells
 Balance time = 15 s:
 (RCB=2, move=12, ghosts=1)

- Balance across processors, static or dynamic
- Geometric method: recursive coordinate bisection (RCB)
- Weighted by cell count or molecules or CPU

In-Situ Visualization

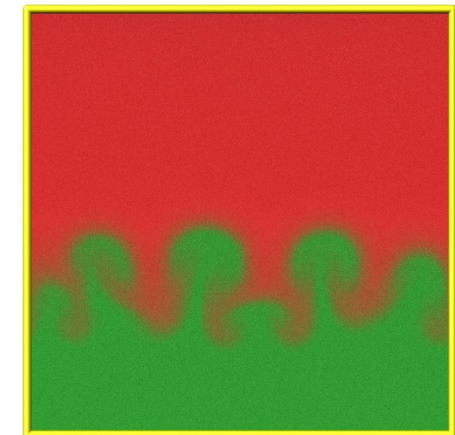
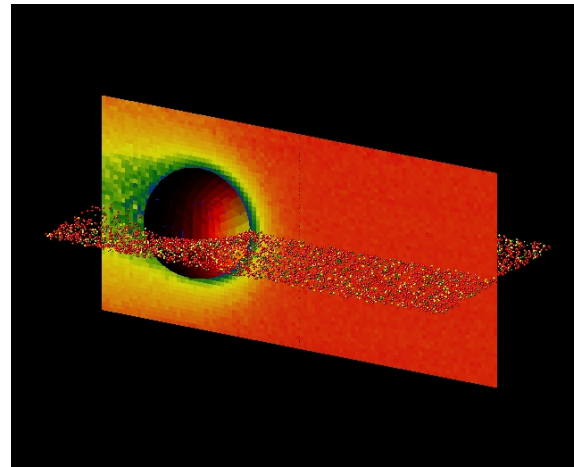
Not a replacement for interactive viz, but ...
Quite useful for **debugging** & quick analysis
At end of simulation (or during), instant movie

Render a JPG snapshot every N time steps:

- Each processor starts with blank image (1024x1024)
- Processor draws its cells/surfaces/molecules with depth-per-pixel
- Merge pairs of images, keep the pixel in front, recurse
- Draw is parallel, merge is logarithmic (like MPI Allreduce)

Images are ray-traced quality

Paraview (<http://www.paraview.org>) has also implemented in-situ.



Aiming for MPI+X via Kokkos

- What is Kokkos:
 - Programming model in development at Sandia
 - C++ template library
 - Open-source
 - Stand-alone
- Goal: write application kernels only once, and run them efficiently on a wide variety of hardware platforms
- Two major components:
 - Data access abstraction via Kokkos arrays optimal layout & access pattern for each device: GPU, Xeon Phi, etc.
 - Parallel dispatch of small chunks of work auto-mapped onto back-end languages: CUDA, OpenMP, etc.

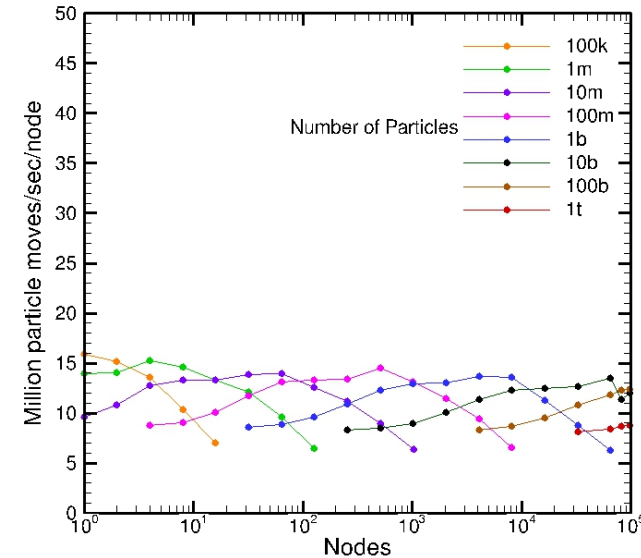
SPARTA Benchmarking

- Flow in a closed box
 - Stress test for communication
 - No preferred communication direction
 - 3D regular grid, 10^4 - 10^{11} (**0.1 trillion**) grid cells
 - 10 molecules/cell, 10^5 - 10^{12} (**1 trillion**) molecules
- Effect of threading
 - **2 threads/core = 1.5 speed**
 - **4 threads/core = 2x speed**

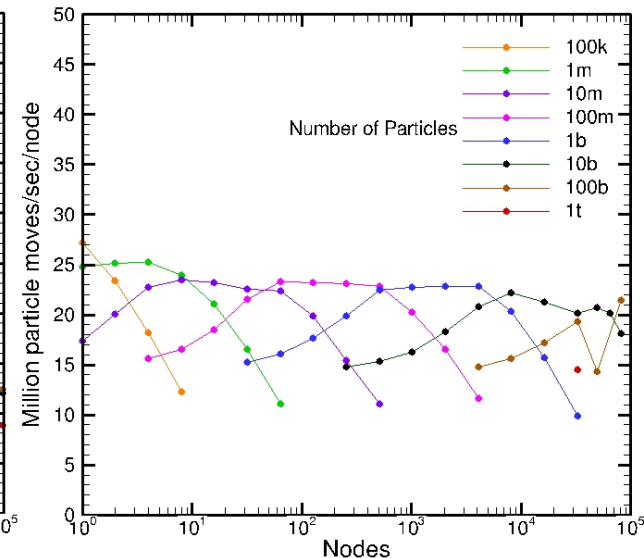


SPARTA Benchmarking

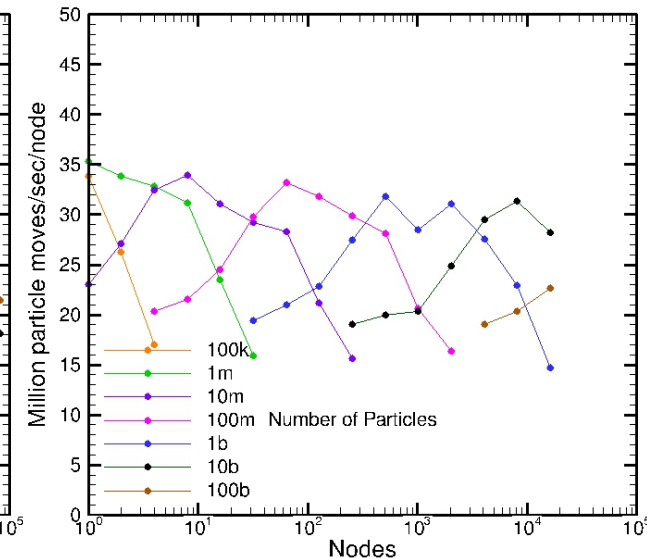
16 cores/node
1 task/core



16 cores/node
2 tasks/core



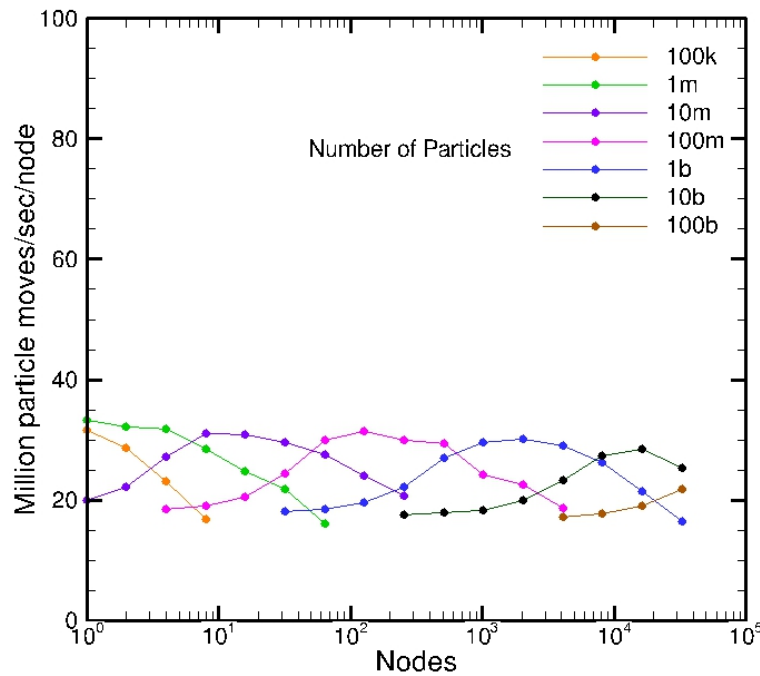
16 cores/node
4 tasks/core



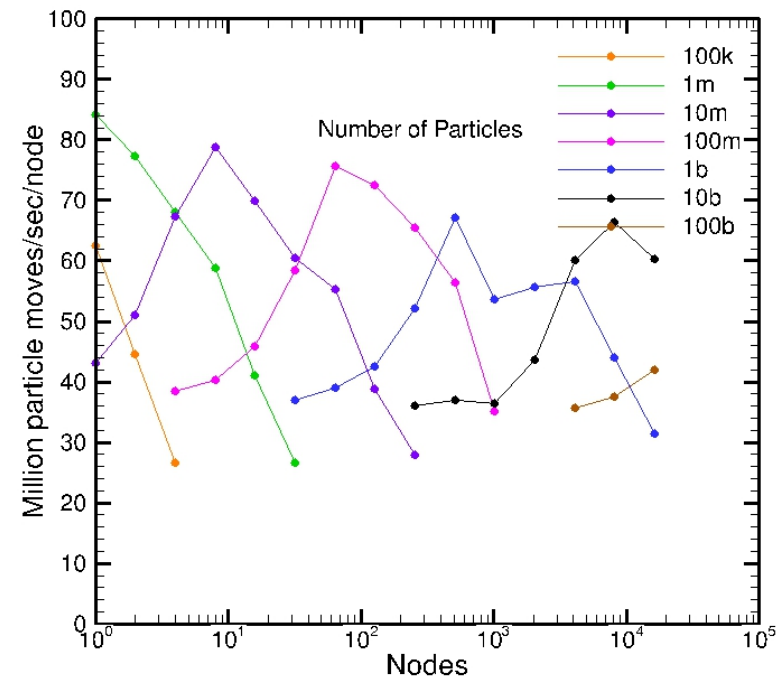
- Weak scaling indicates, 10% peak performance reduction from 1 to 10^6 cores
- 2 tasks/core gives 1.5x speedup, 4 tasks/core gives 2x speedup
- A total of **1 trillion molecules** can be simulated on **one third** of the BG/Q
- Maximum number of tasks is 2.6 million

SPARTA Benchmarking (FM)

16 cores/node, 1 task/core



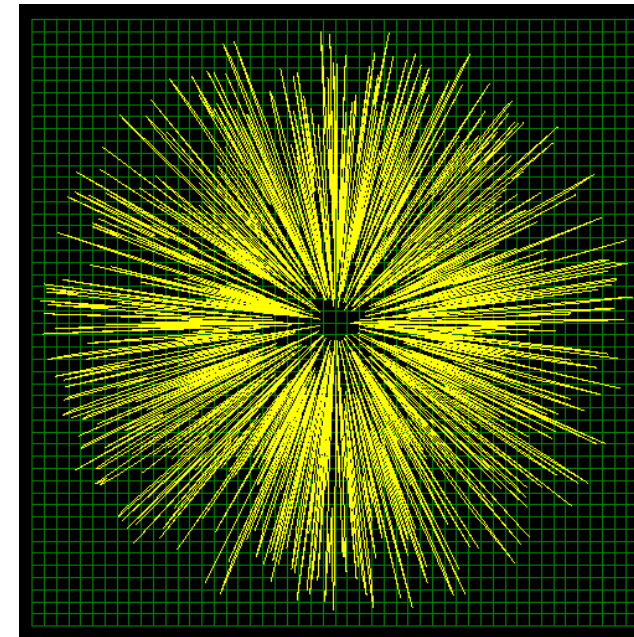
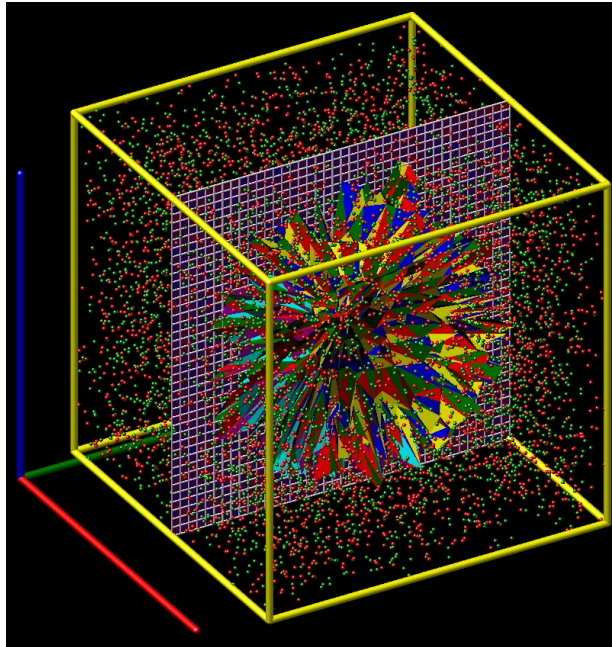
16 cores/node, **4** tasks/core



- Free-molecular (FM) calculations stress-test for communications
- 2x speedup compared to collisional

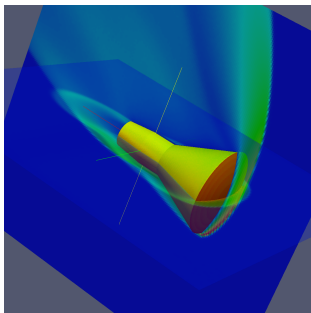
Simulation of Complicated Shapes

- SPARTA now computes all the cut cell volumes, identifies any split cells, colors all grid cells as inside, outside, or cut/split.
- Each surface in a split cell is tagged by which split volume it belongs to, which will be needed for tracking particles into the split cells.
- Infinitely thin surfaces are detected and correctly dealt with during molecular advection.

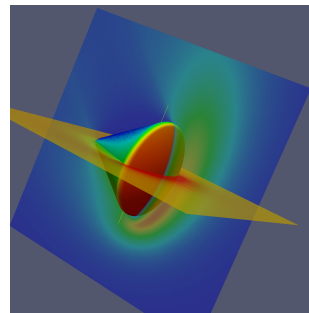


Simulations of Re-entry Vehicles

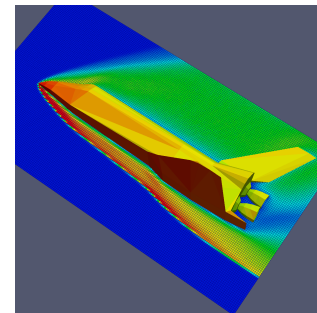
Gemini
1961-1966



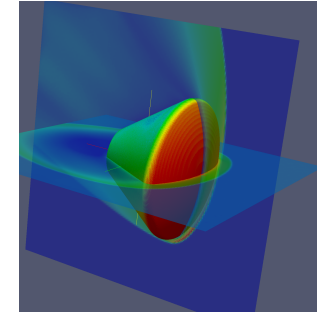
Apollo
1963-1972



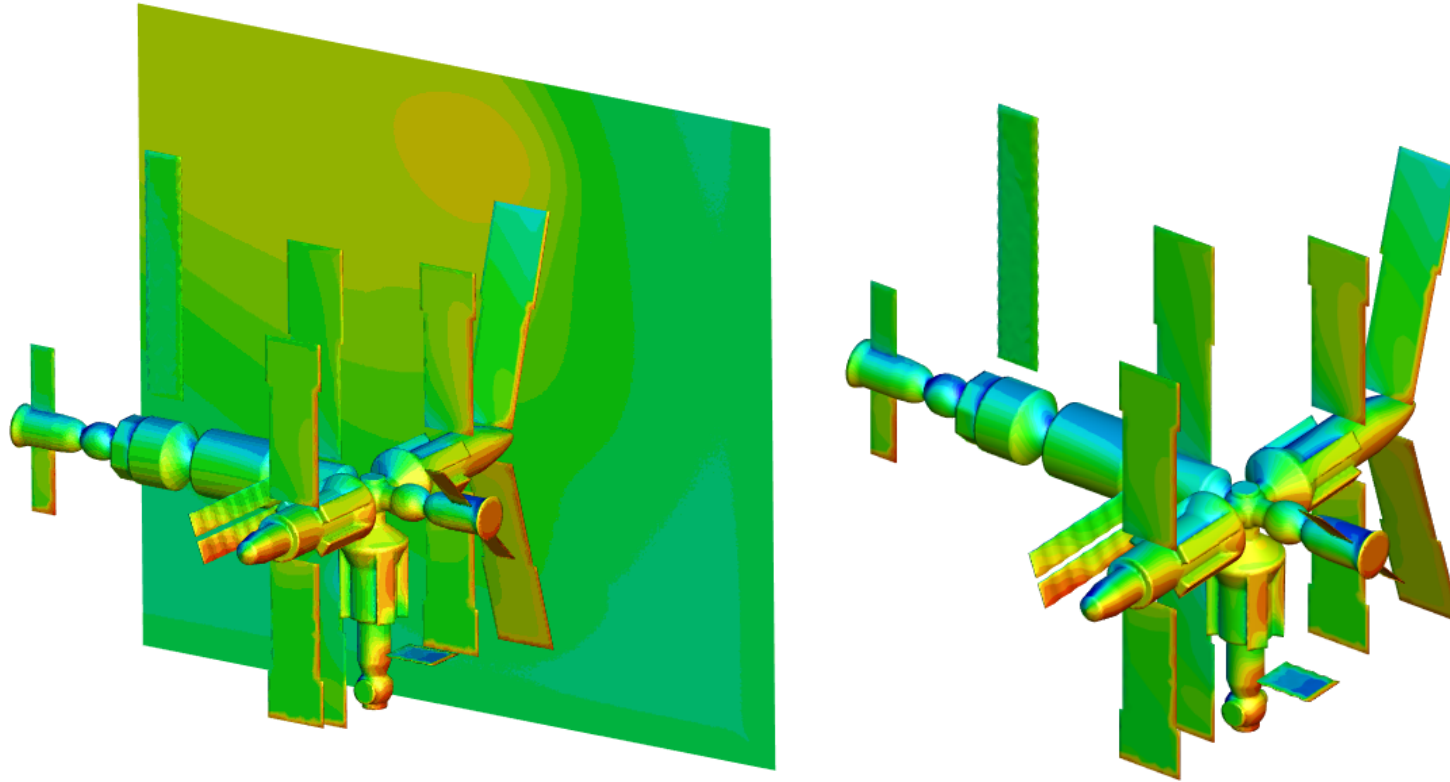
Space Shuttle
1981-2011



Orion
2014-?



Simulation of Mir Space Station



Mir Space Station

Grid generation (10^7 cells) completed in 0.3 seconds on 16 processors
Geometry comprises multiple “water-tight” bodies

Verification test cases

- Sonine polynomials
- Closed box
 - Collision frequency
 - Inflow boundary conditions
 - Internal energy relaxation
 - Chemical reactions
- Axisymmetric flow
- Flow over a sphere

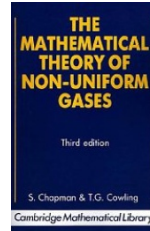
Near-Equilibrium: Chapman-Enskog (CE) Theory



Sydney
Chapman



David
Enskog



$$f = f^{(0)}(1 + \Phi^{(1)} + \Psi^{(1)}) \quad f^{(0)} = (n/\pi^{3/2} c_m^3) \exp[-\tilde{c}^2]$$

$$c_m = \sqrt{2k_B T/m} \quad \tilde{\mathbf{c}} = \mathbf{c}/c_m \quad \mathbf{c} = \mathbf{v} - \mathbf{u}$$

$$\Phi^{(1)} = -\left(8/5\right) \tilde{A}[\tilde{c}] \tilde{\mathbf{c}} \cdot \tilde{\mathbf{q}} \quad \Psi^{(1)} = -2 \tilde{B}[\tilde{c}] (\tilde{\mathbf{c}} \circ \tilde{\mathbf{c}} : \tilde{\tau})$$

$$\tilde{A}[\tilde{c}] = \sum_{k=1}^{\infty} (\textcolor{red}{a_k/a_1}) S_{3/2}^{(k)}[\tilde{c}^2] \quad \tilde{B}[\tilde{c}] = \sum_{k=1}^{\infty} (\textcolor{red}{b_k/b_1}) S_{5/2}^{(k-1)}[\tilde{c}^2]$$

$$C_p = (5/2)(k_B/m) \quad \text{Pr} = (2/3)(\textcolor{blue}{\mu_{\infty}/\mu_1})(\textcolor{blue}{K_1/K_{\infty}})$$

- Chapman and Enskog analyzed Boltzmann collision term
 - Perturbation expansion using Sonine polynomials
 - Near equilibrium, appropriate in continuum limit
- Determined velocity distribution
 - Distribution “shape”: Sonine polynomial coeffs. $a_k/a_1, b_k/b_1$
 - Values for all Inverse-Power-Law (IPL) interactions
 - Maxwell and hard-sphere are special cases

Gallis M. A., Torczynski J. R., Rader D. J., “Molecular Gas Dynamics Observations of Chapman-Enskog Behavior and Departures Therefrom in Nonequilibrium Gases”, *Physical Review E*, 69, 042201, 2004.

Extracting CE Parameters from DSMC

$$\frac{a_k}{a_1} = \sum_{i=1}^k \left(\frac{(-1)^{i-1} k! (5/2)!}{(k-i)! i! (i+(3/2))!} \right) \left(\frac{\langle \tilde{c}^{2i} \tilde{c}_x \rangle}{\langle \tilde{c}^2 \tilde{c}_x \rangle} \right)$$

$$\tilde{\mathbf{c}} = \frac{\mathbf{v} - \mathbf{V}}{c_m}$$

$$\frac{b_k}{b_1} = \sum_{i=1}^k \left(\frac{(-1)^{i-1} (k-1)! (5/2)!}{(k-i)! (i-1)! (i+(3/2))!} \right) \left(\frac{\langle \tilde{c}^{2(i-1)} \tilde{c}_x \tilde{c}_y \rangle}{\langle \tilde{c}_x \tilde{c}_y \rangle} \right)$$

$$c_m = \sqrt{\frac{2k_B T}{m}}$$

DSMC moments of velocity distribution function

- Temperature T , velocity \mathbf{V}
- Higher-order moments

DSMC values for VSS molecules (variable-soft-sphere)

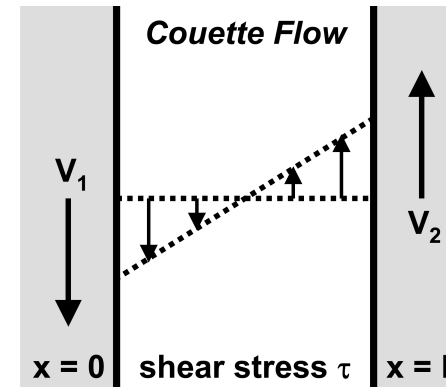
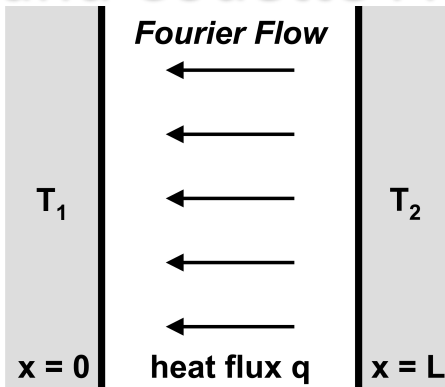
- Sonine-polynomial coefficients: a_k/a_1 and b_k/b_1
- Applicable for arbitrary Kn_L , Kn_q , Kn_τ

Quantifying Non-Equilibrium Fourier and Couette Flow



Joseph Fourier

$$q = -K \frac{\partial T}{\partial x}$$



Maurice Couette

$$\tau = \mu \frac{\partial v}{\partial x}$$

Investigate transport in gas between parallel plates

- Fourier flow: heat conduction in stationary gas
- Couette flow: momentum transport in isothermal shear flow

Apply DSMC to Fourier flow and Couette flow

- Heat flux, shear stress: one-dimensional, steady

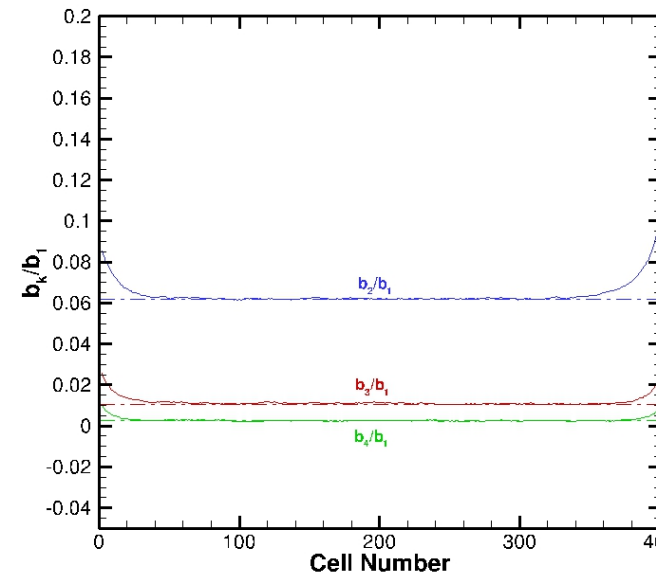
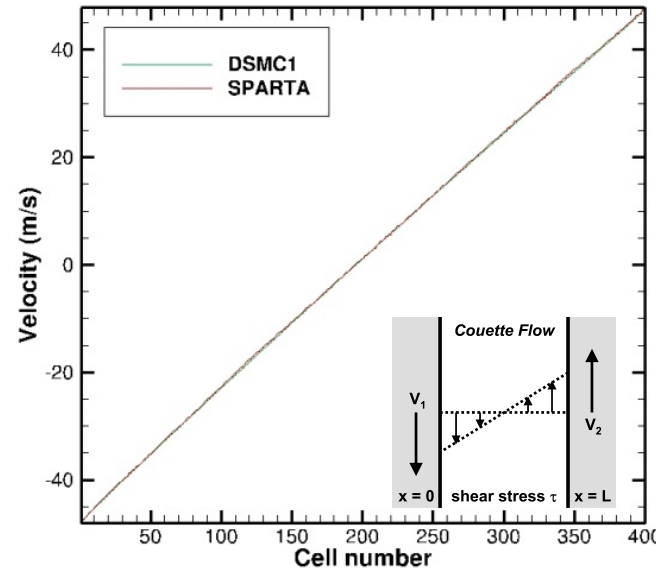
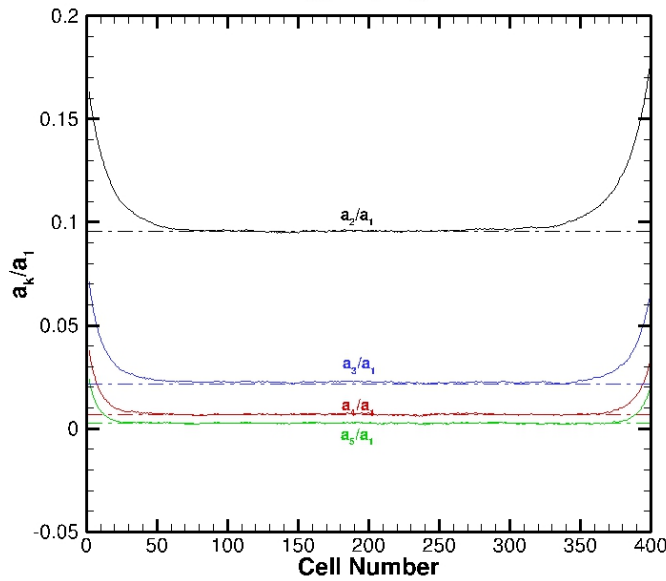
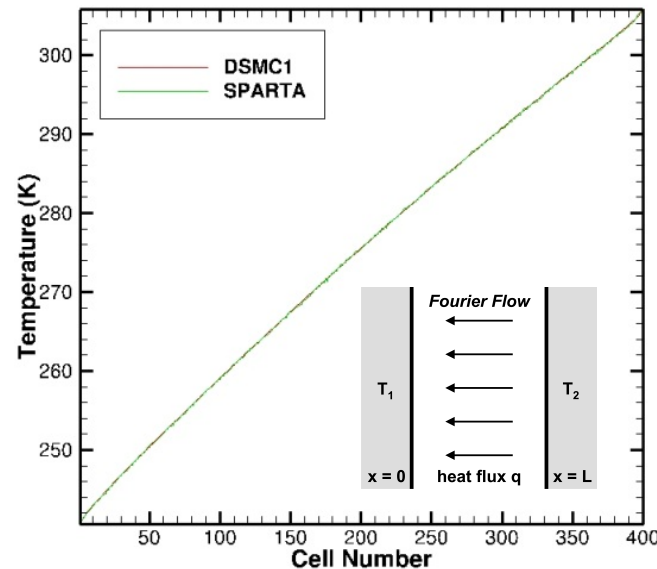
Compare DSMC to analytical “normal solutions”

- Normal: outside Knudsen layers
- Solutions: Chapman-Enskog (CE), Moment-Hierarchy (MH)

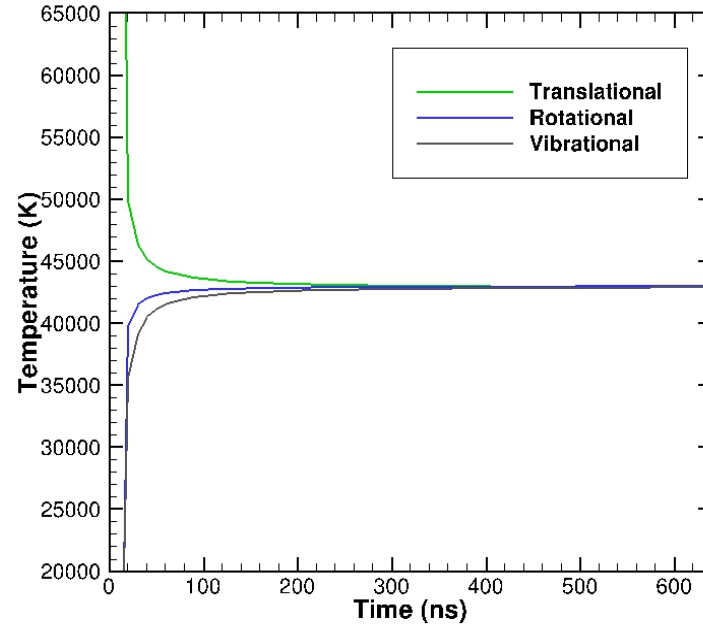
Verify DSMC accuracy at arbitrary heat flux, shear stress

- Thermal conductivity, viscosity; velocity distribution

Sonine Polynomial Coefficients

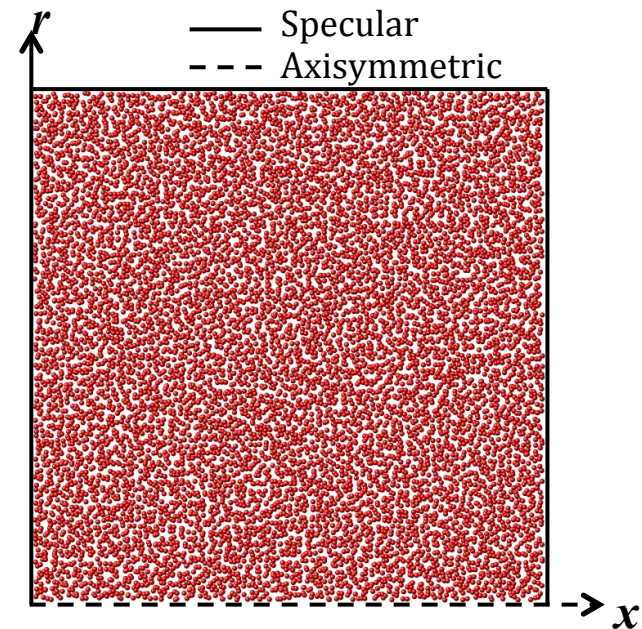
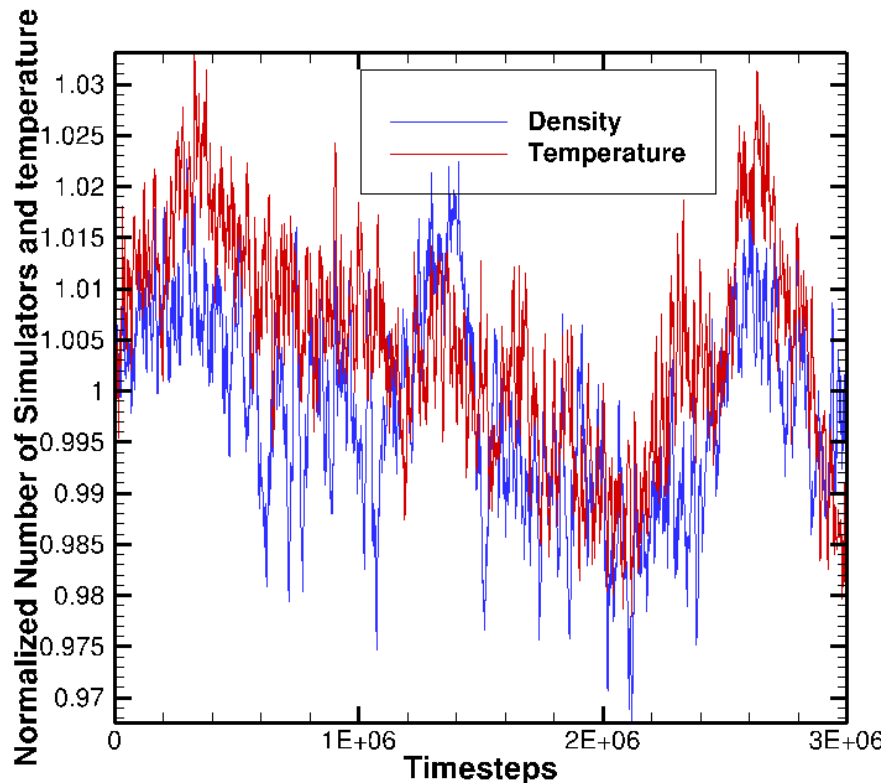


Internal Energy Relaxation



Molecules of a diatomic gas are allowed to perform energy exchange through successive molecular collisions (specular walls). Initially the molecules are assumed to have all their energy in the translational mode. Eventually, all three energy modes, translational, rotational and vibrational, reach thermal equilibration.

Axisymmetric Flow



Validation test cases

- Comparisons with experimental data from:
 - CUBRIC Lens
 - 25/55 deg biconic (2D-axisymmetric)
 - Hollow cylinder flare (2D-axisymmetric)
 - SR3
 - 70 deg Cone (2D-axisymmetric)
 - Flat plate (2D)

Simulations performed by A. Klothakis and I. Nikolos, *Modeling Of Rarefied Hypersonic Flows Using The Massively Parallel DSMC Kernel “Sparta”*, 8th GRACM International Congress on Computational Mechanics, Volos, Greece, July 12–15, 2015

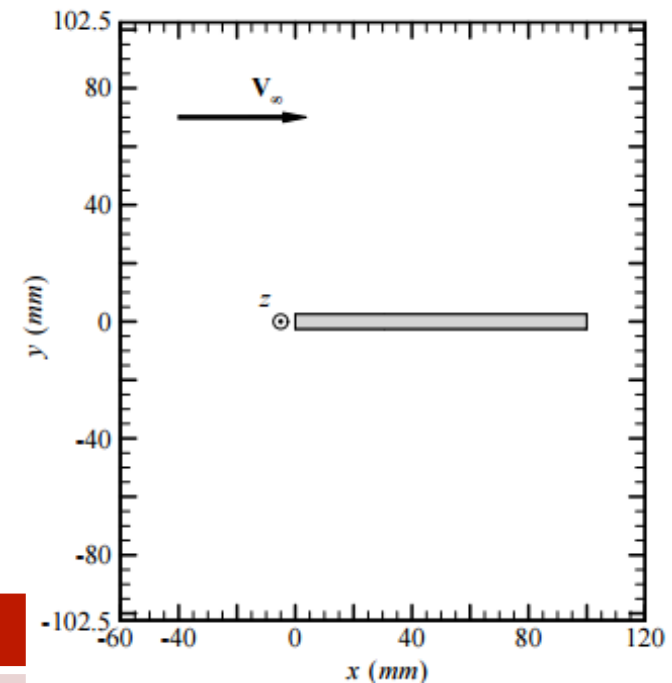
Hypersonic flow around a flat plate

- Geometry: Flat plate

Length : 100mm

Height : 50mm

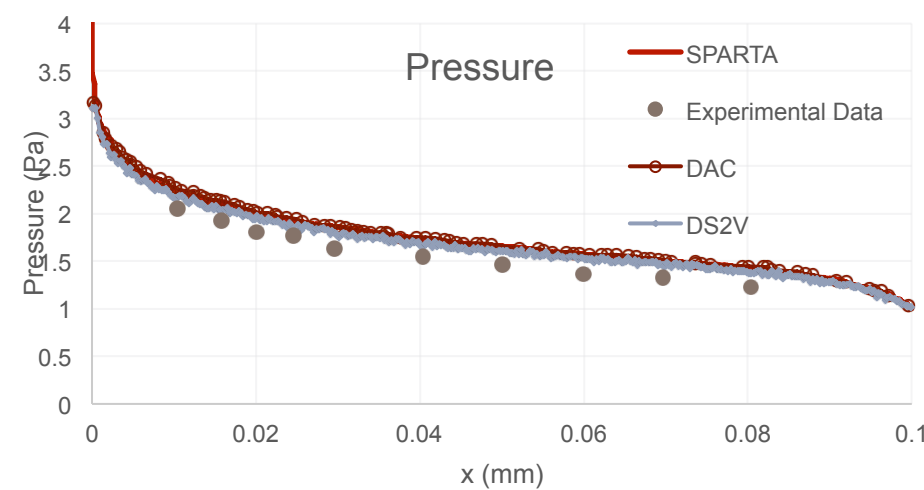
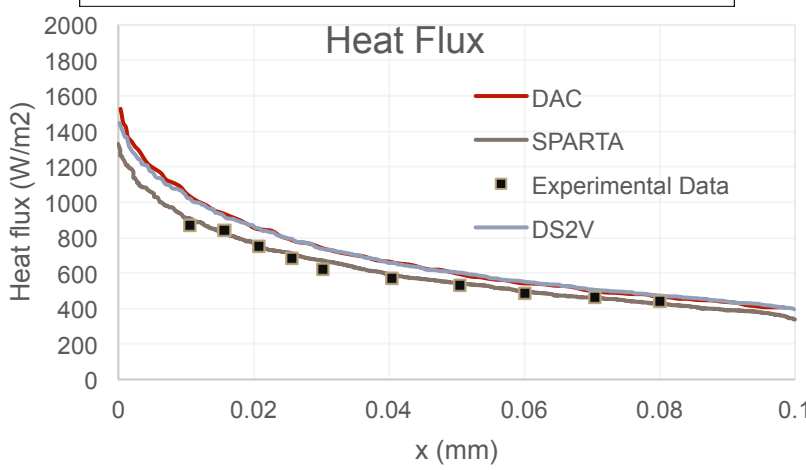
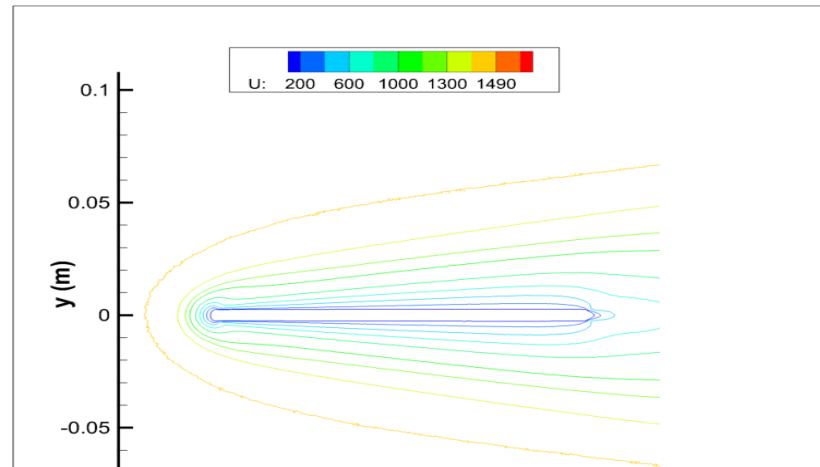
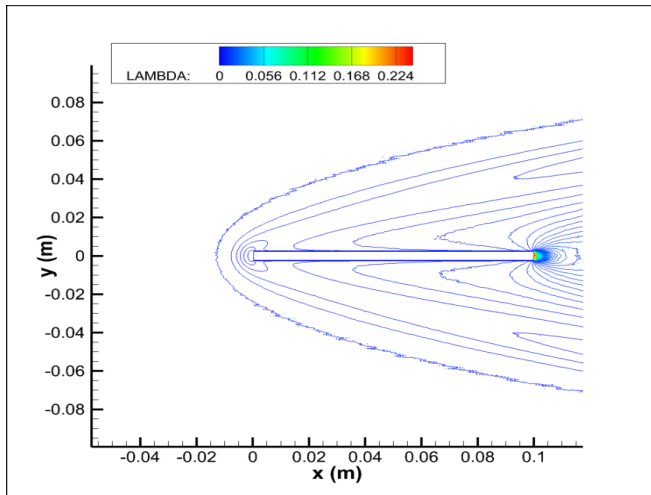
- Flowfield Dimensions : 180mm x 205mm
- Grid size: 360 x 410 cells
- Cell size: 0.5mm x 0.5mm
- $\lambda=1.6$ mm



Flow conditions			
V_∞	T_∞	T_w	Density
1504	13.32	290	$3,716 \cdot 10^{20}$

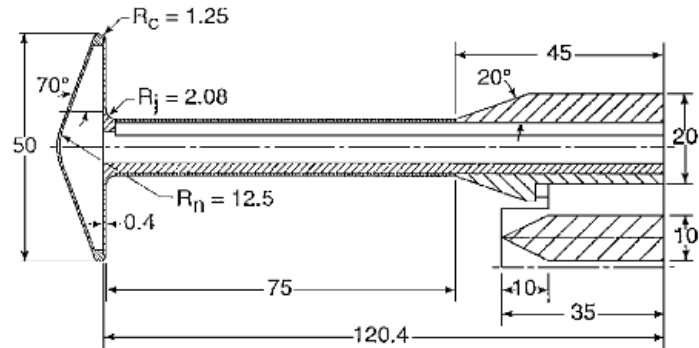
Allègre, J., Raffin, M., Chpoun, A., Gottesdiener, L. (1992), "Rarefied Hypersonic Flow over a Flat Plate with Tuncated Leading Edge", *Progress in Astronautics and Aeronautics*, pp. 285-295

Hypersonic flow around a flat plate



Hypersonic flow around a 70-degree blunt cone

- Geometry: AGARD Group Mars Pathfinder
- Flowfield dimensions: 10cm x 15cm
- Grid: 600x600 cells, 2-level 10x10 cells around the cone area

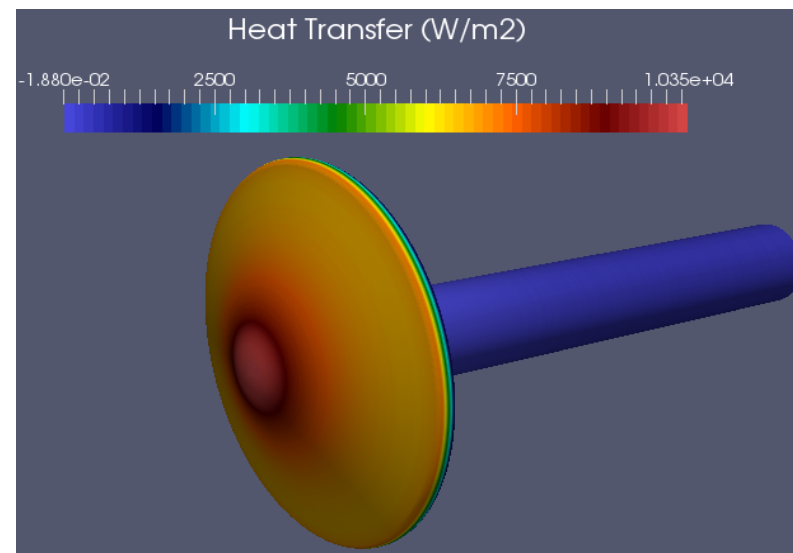
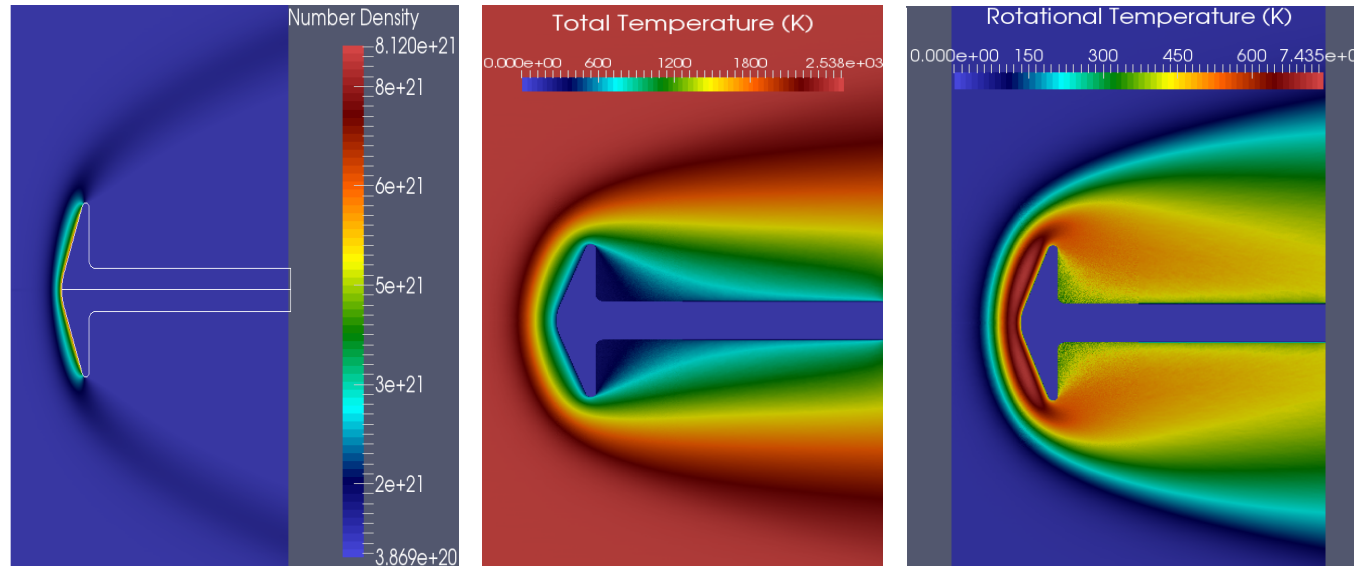


Blunt cone geometry
(Dimensions in mm)

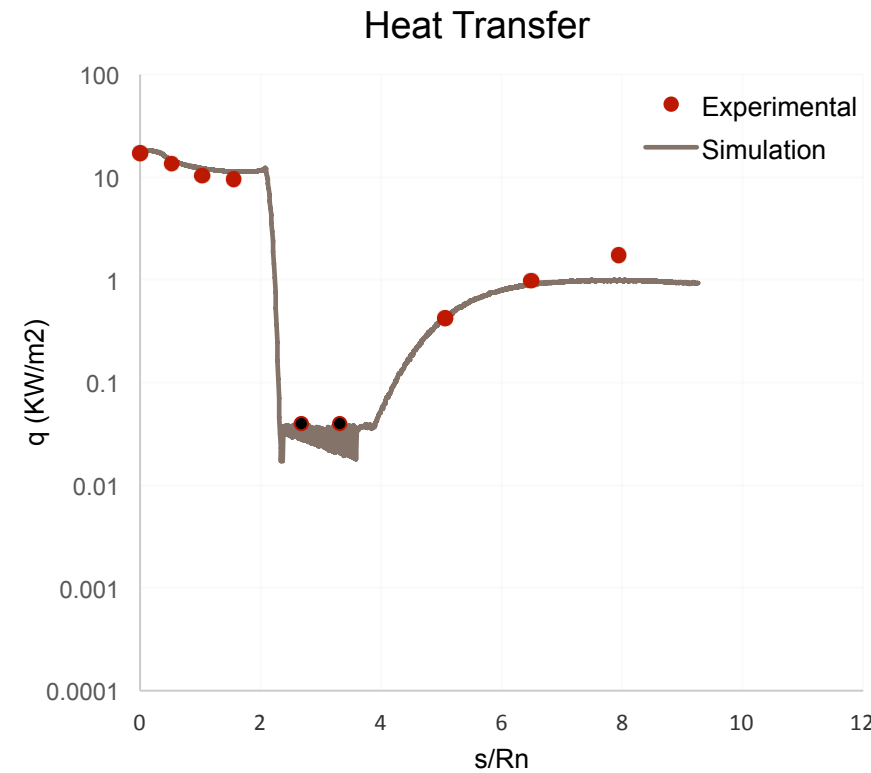
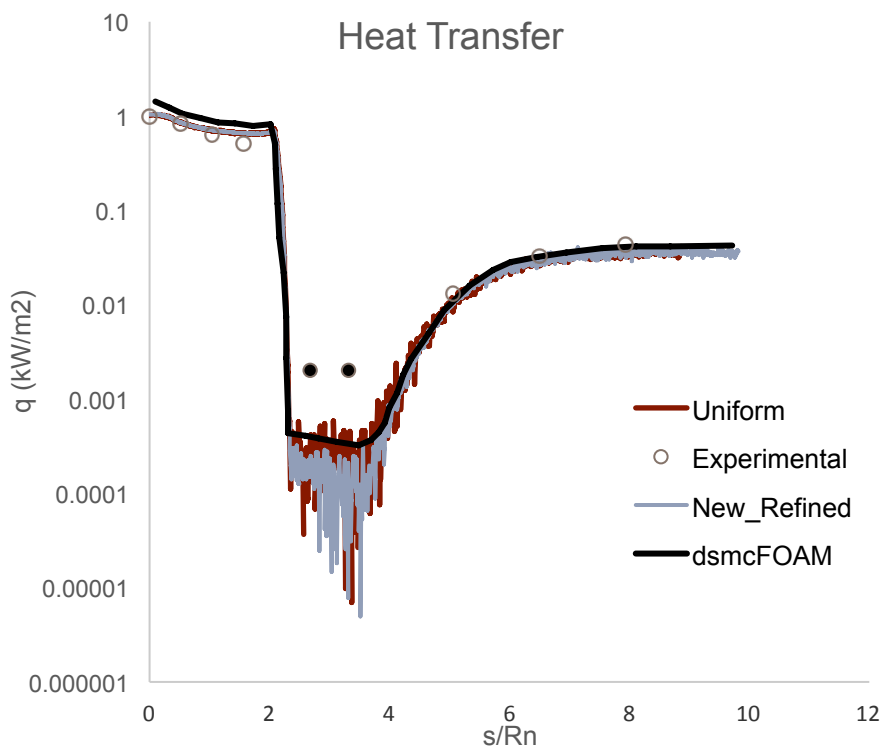
Flow conditions	Gas	Ma	T ₀	P ₀	Re
1	N ₂	20.2	1100	3.5	1420
2	N ₂	20	1100	10	4175

Allègre, J., Bisch, D., Lengrand, J. C. (1997), "Experimental Rarefied Heat Transfer at Hypersonic Conditions over a 70-Degree Blunted Cone", Journal of Spacecraft and Rockets, Vol. 34, No. 6, pp. 724-728.

Hypersonic flow around a 70-degree blunt cone

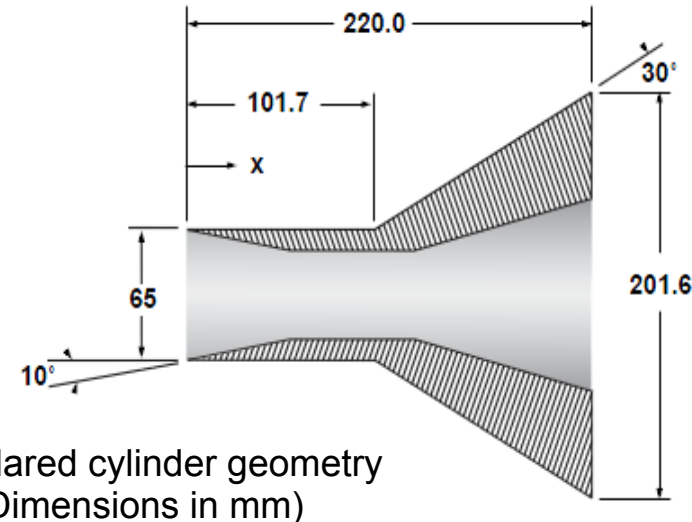


Hypersonic flow around a 70-degree blunt cone



Hypersonic flow around a flared cylinder

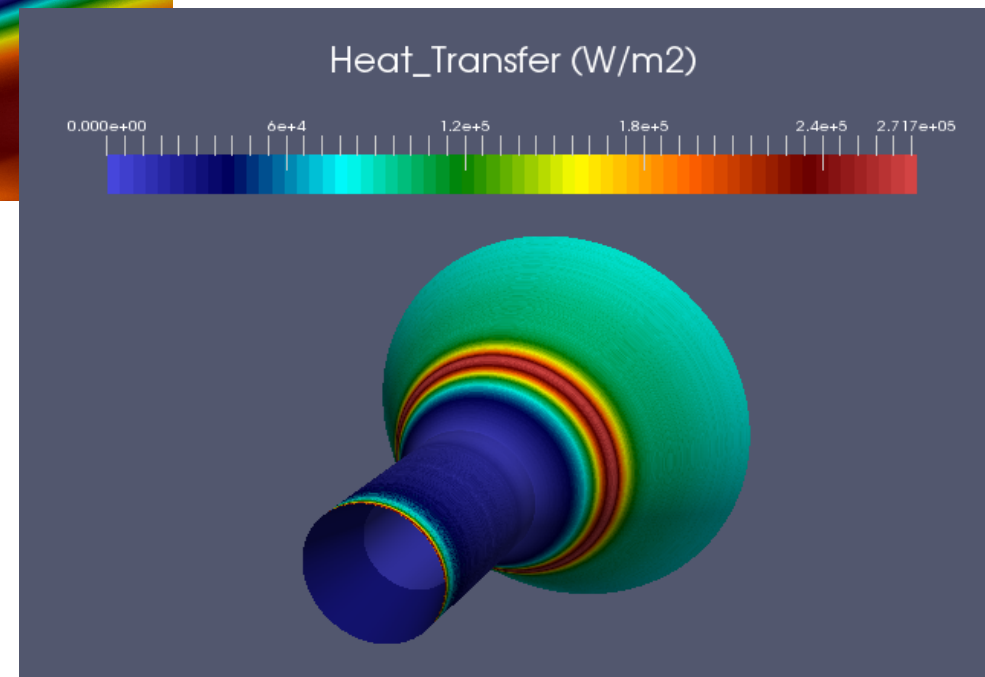
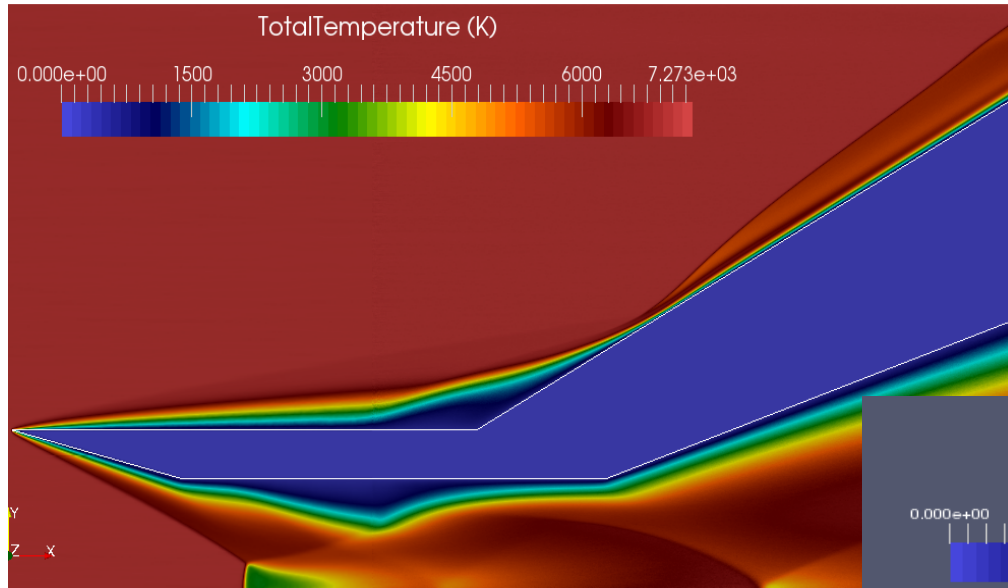
- Flowfield dimensions: 22cm x 12cm
- Grids : Uniform 1000x1800 cells, 2-
Level 957x440 cells second level
10x10 cells



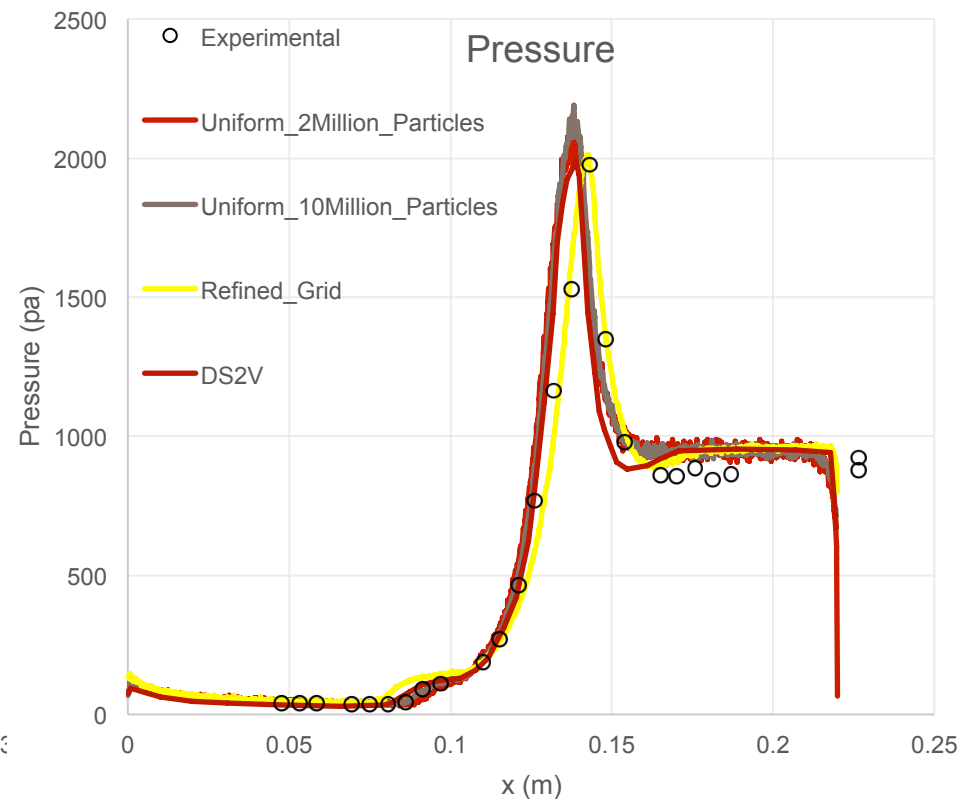
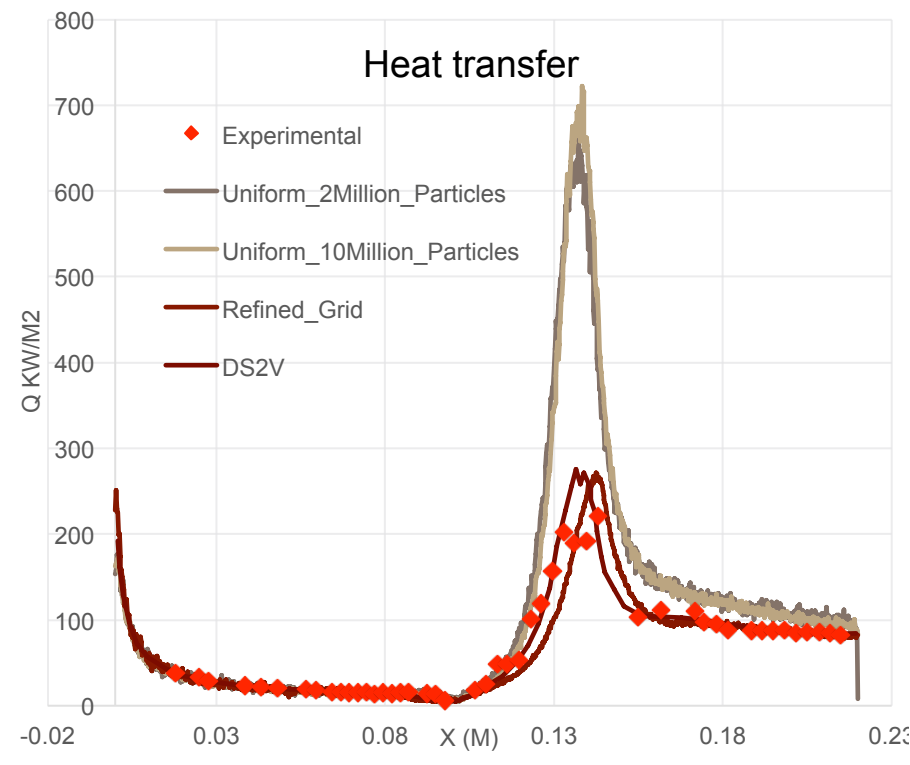
Conditions	Flow Velocity (m/s)	Number Density, m^{-3}	Flow temperature (K)	Gas	Surface Temperature (K)
LENS Run 11	2484	3.78×10^{21}	95.6	N_2	297.2

Holden, M., Harvey, J., Wadhams, T., and MacLean, M., "A Review of Experimental Studies with the Double Cone Configuration in the LENS Hypervelocity Tunnels and Comparisons with Navier-Stokes and DSMC Computations," AIAA 2010-1281, 48th AIAA Aerospace Sciences Meeting, Orlando, FL, January 4-7, 2010.

Hypersonic flow around a flared cylinder

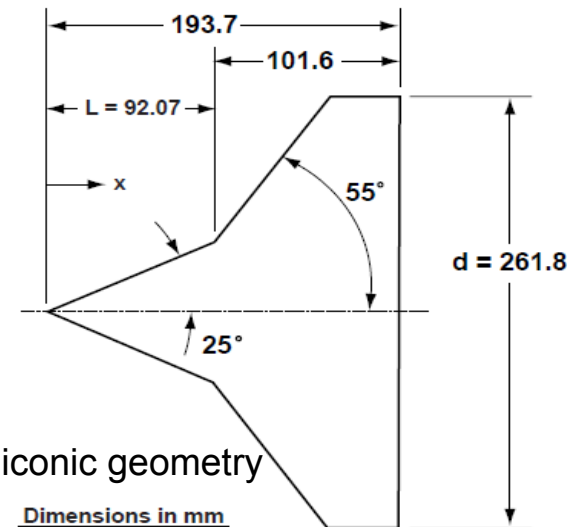


Hypersonic flow around a flared cylinder



Hypersonic flow around a 25/55 degree biconic

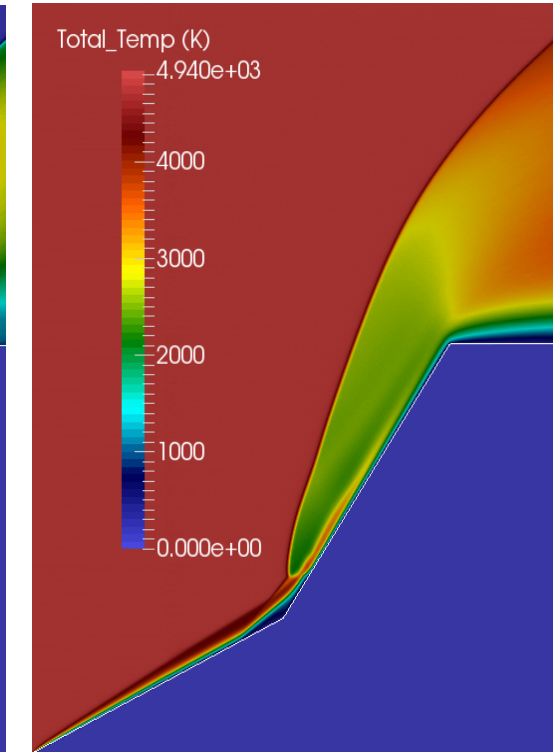
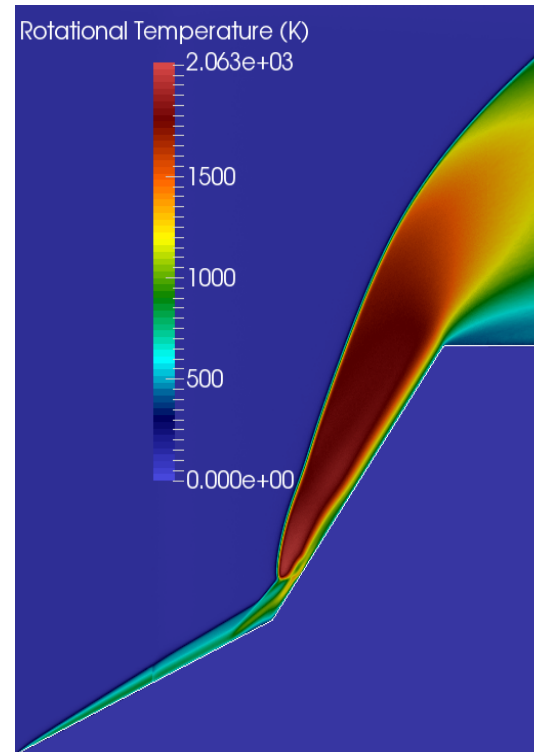
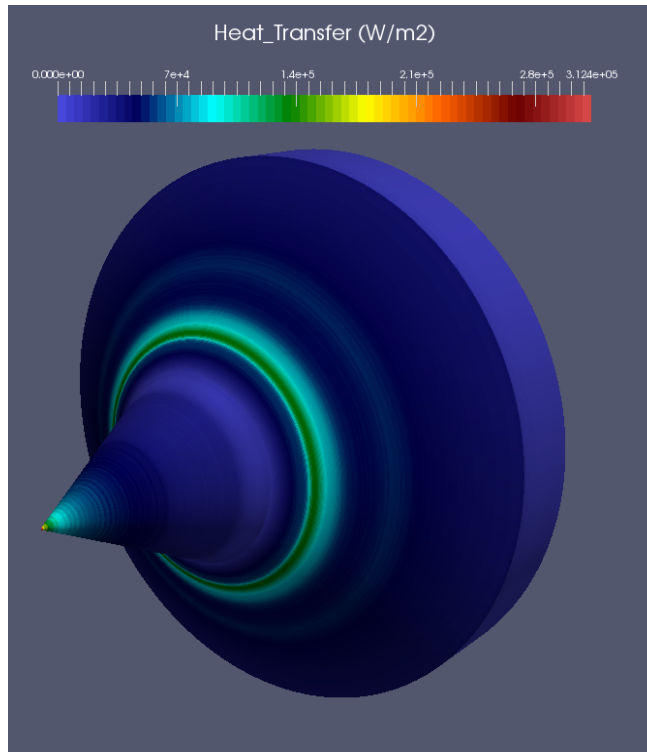
- Flowfield dimensions: 22cm x 50cm
- Grid : 2 level grid, first level 870x870 cells, second level 10x10 cells refinement on the first level, second level starts from 5cm after the biconic's leading edge and ends at the end of the biconic's surface.



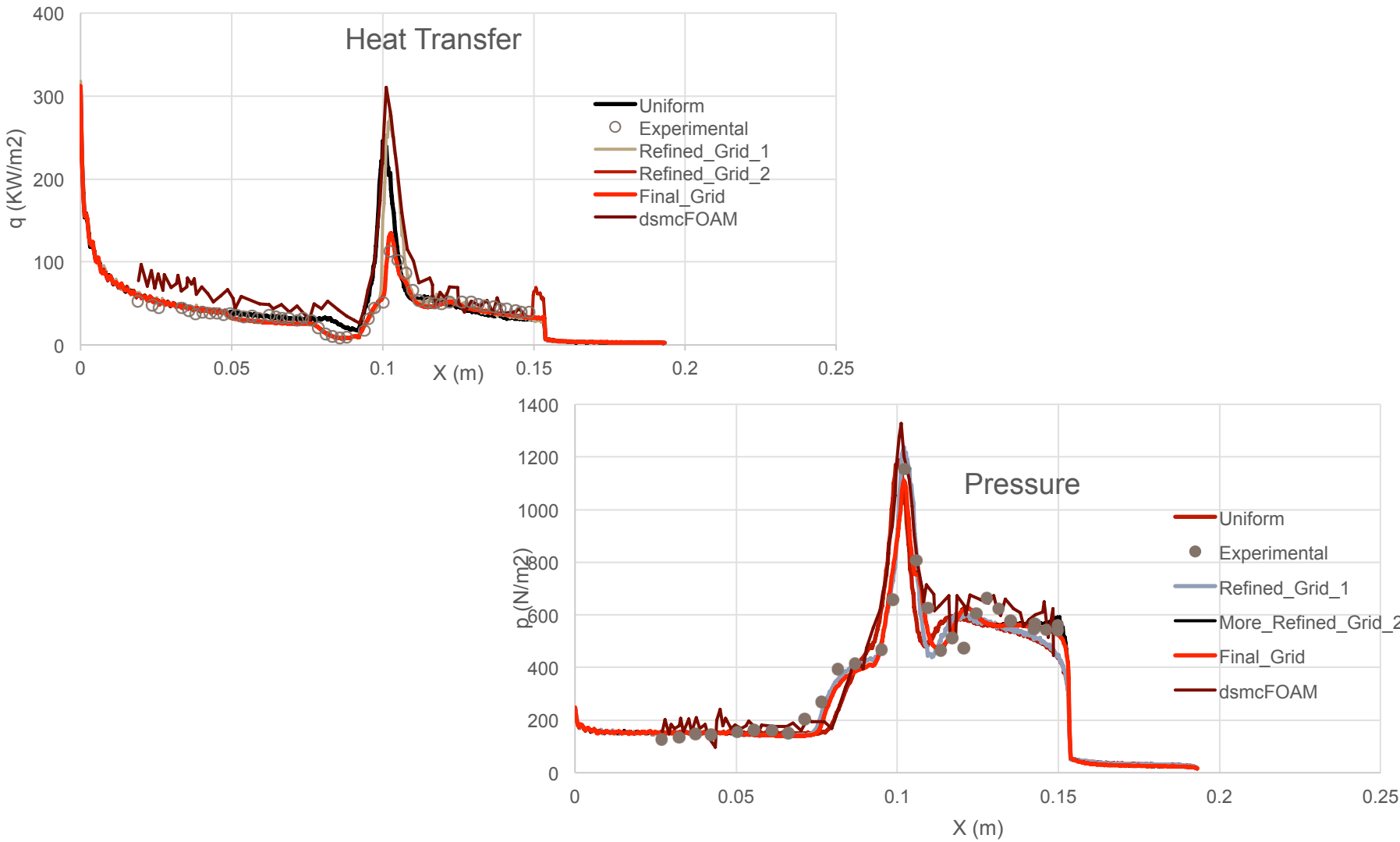
Conditions	Flow Velocity (m/s)	Number Density, m^{-3}	Flow temperature (K)	Gas	Surface Temperature (K)
CUBRC Run 7	2072.6	3.0×10^{18}	42.61	N_2	297.2

Holden, M., Harvey, J., Wadhams, T., and MacLean, M., "A Review of Experimental Studies with the Double Cone Configuration in the LENS Hypervelocity Tunnels and Comparisons with Navier-Stokes and DSMC Computations," AIAA 2010-1281, 48th AIAA Aerospace Sciences Meeting, Orlando, FL, January 4-7, 2010.

Hypersonic flow around a 25/55 degree biconic



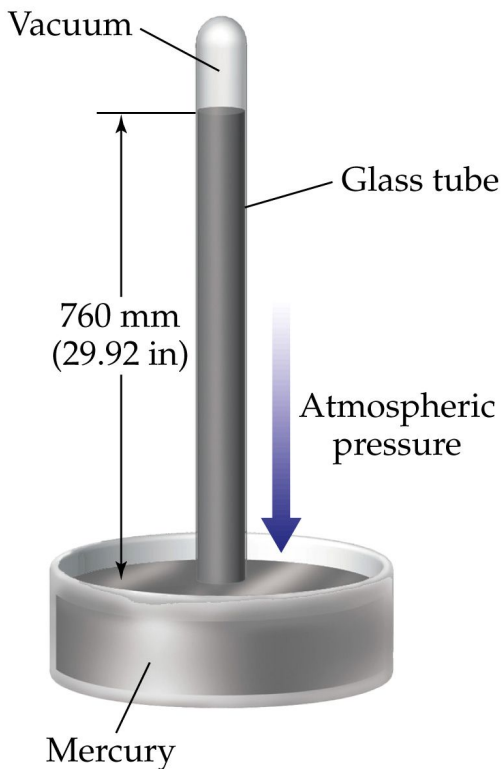
Hypersonic flow around a 25/55 degree biconic



Torricelli's Mercury Barometer



Evangelista Torricelli



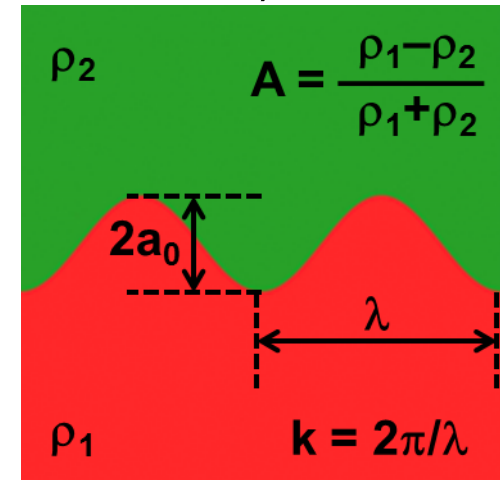
In 1643 Torricelli invented the barometer

The mercury column stands at 0.76 m indicating that
atmospheric pressure can support 10 m (=14x0.76 m) of water



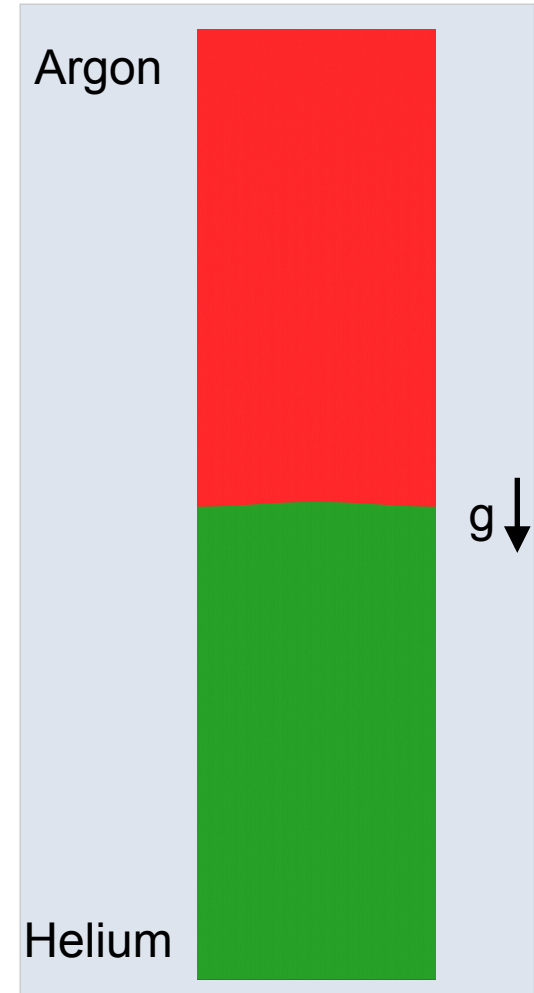
Why DSMC for Rayleigh-Taylor Instability?

- DSMC provides a molecular-level description of the hydrodynamic processes that may be physically more realistic for **large accelerations and chemically reacting flows**
- DSMC inherently accounts for transport properties
- The DSMC method offers the potential to identify the impact of molecular level effects (e.g. rotational and vibrational energy exchange, gas-phase chemical reactions, and gas-surface interactions) on hydrodynamic instabilities.
- Typical DSMC simulation characteristics:
 - Physical Domain: 1 mm x 4 mm (ICF-pellet size domain)
 - # Cells: 4 billion
 - # Particles: 400 billion
 - # Cores: 1/4- 1/2 million
 - Run time: 30hrs (=900, 1800 CPU years)
 - Time steps: $200,000 \times 0.1 \text{ ns} = 20 \text{ } \mu\text{s}$

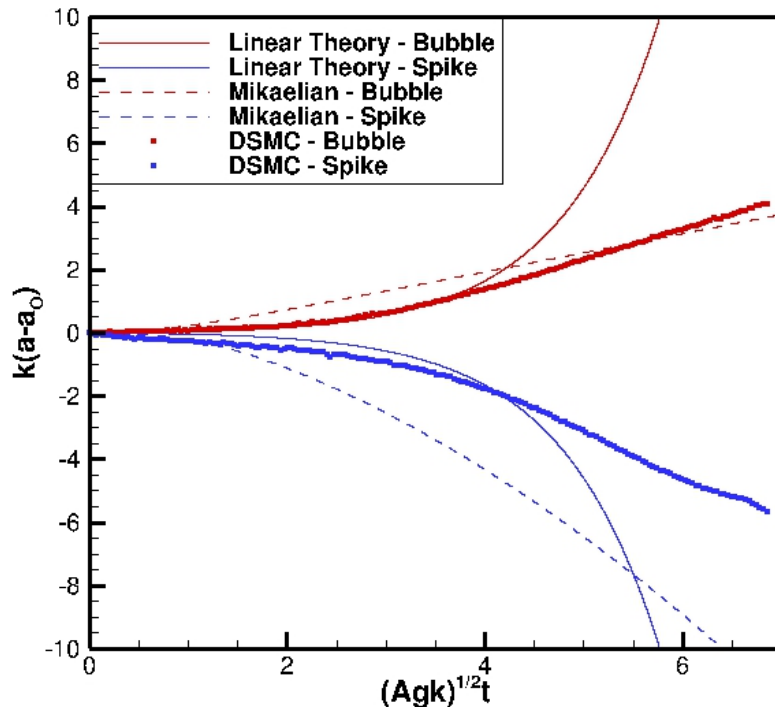


DSMC Simulations of the Rayleigh-Taylor Instability in Gases

- The interface between argon (red) and helium (green) gases is slightly perturbed:
 $\lambda = 0.001m, a = 0.00001m$
- Initial state hydrodynamic equilibrium
- Acceleration of the system excites the RTI
 - Initially, **thermal fluctuations and diffusion** perturb the interface
 - The initial perturbation amplitude grows exponentially
 - A second growth stage occurs at the most unstable wavelength, also forming **“bubbles”** and **“spikes”**
 - Additional instabilities breakup the larger structures, resulting **in turbulent and chaotic mixing of the gases**

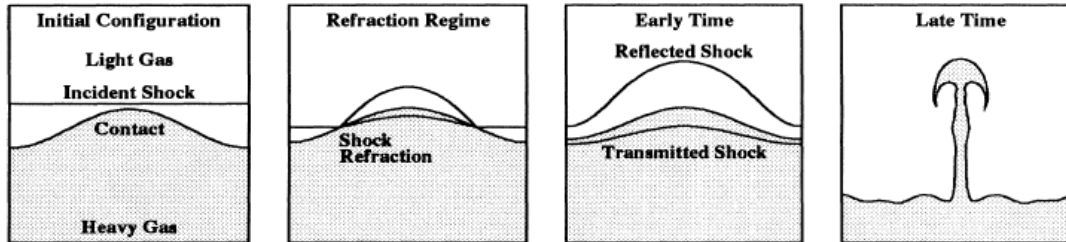


Development of 0.001 m Wavelength Perturbation

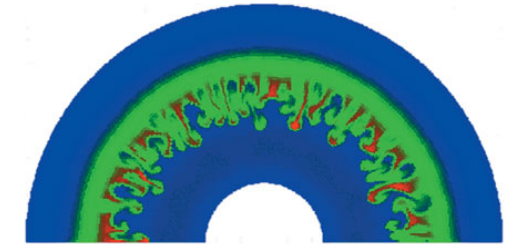


Initial perturbations of a small wavelength develop and grow exponentially. Larger structures appear as the smaller disturbances interact and combine. The structures themselves develop instabilities like the Kelvin-Helmholtz instability, which eventually break up the structures, resulting in turbulent and chaotic mixing of the fluids.

Richtmyer-Meshkov Instability (RMI)



Grove et al., Phys. Rev. Lett., 71(21), 3473 (1993).

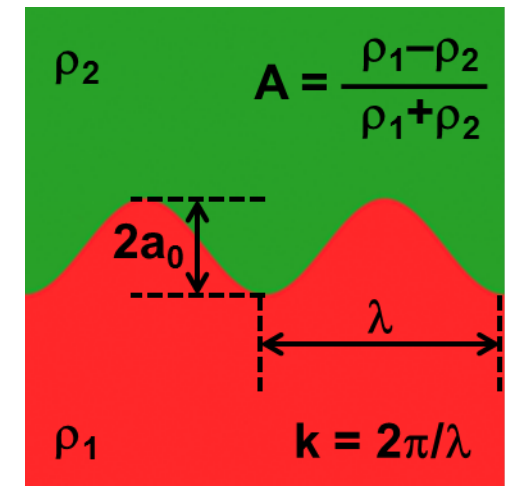


ICF target compression

RMI applications include stellar evolution, inertial confinement fusion, shock-flame interaction

RMI combines multiple fluid-flow phenomena

- Shock transmission and reflection
- Hydrodynamic instabilities
- Linear and nonlinear growth
- Diffusion and turbulent mixing
- Compressibility effects
- Chemical reactions



RMI basic geometry

Simulate RMI using molecular gas dynamics

- Physical conditions that can be achieved
- Computational software & hardware needed

RMI in Gas Mixtures

Physical situation

- Gases: pairs of helium, neon, argon, xenon, air, SF_6
- STP conditions: both gases at 1 atm and 0 °C
- Two-dimensional domain: 0.1 mm × 0.4 mm
- Wavelength, initial amplitude: 0.05 mm, 0.01-0.1 mm

Numerical parameters

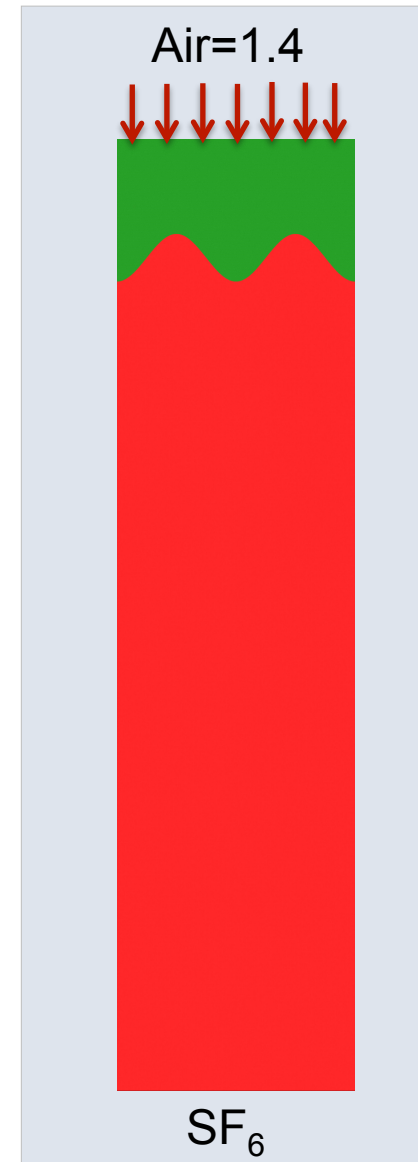
- Mesh: 5 nm, $20,000 \times 80,000 = 1.6$ billion cells
- Molecules: 800 billion molecules (500 per cell)
- Time steps: $200,000 \times 0.01$ ns = 2 μs

Computational aspects

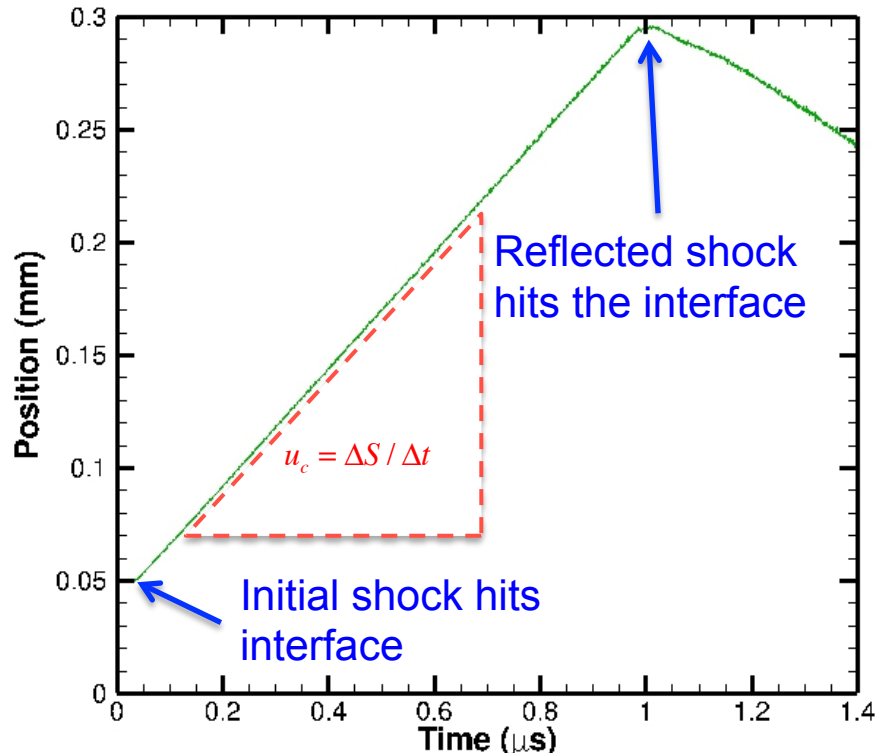
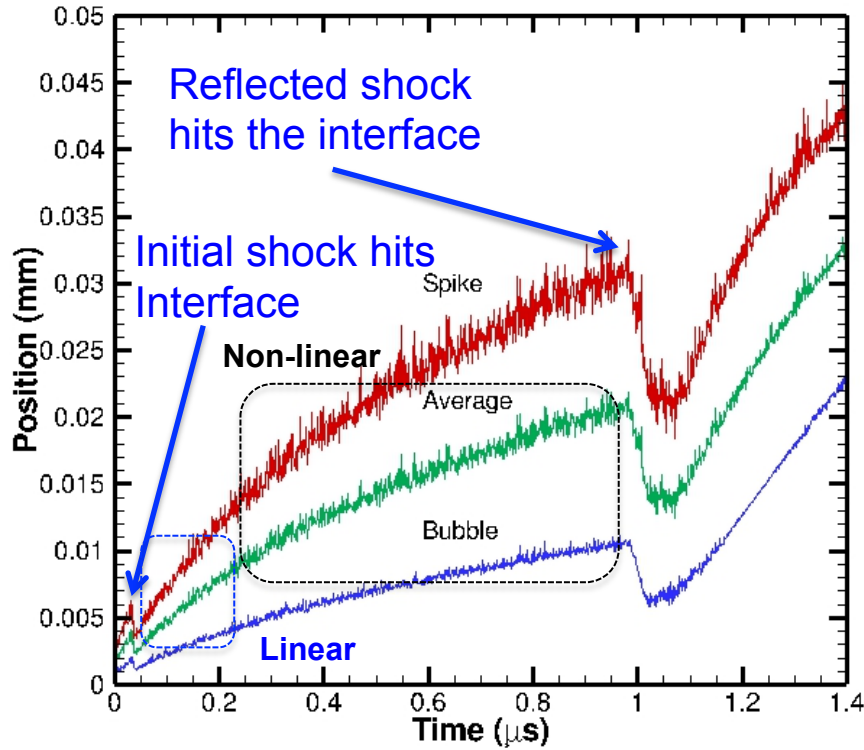
- Platform: Sequoia, 30 hours
- Processors: $\sim \frac{1}{4}$ million cores (16k nodes) (900 years CPU time)

Flow phenomena

- Flow at top is impulsively started and maintained
- Shock wave propagates down and hits interface
- Transmitted and reflected shock waves depart
- Interface moves down and grows thicker



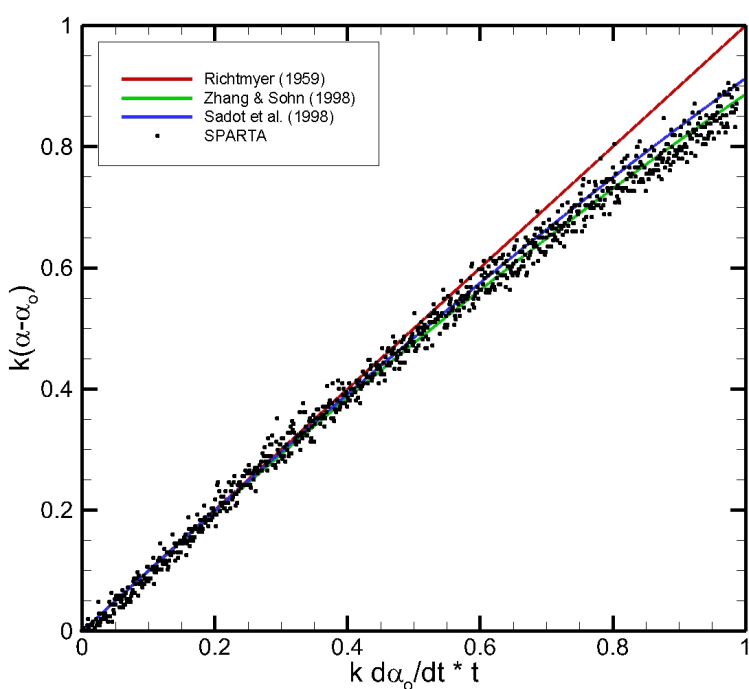
Development of Bubbles and Spikes in RMI



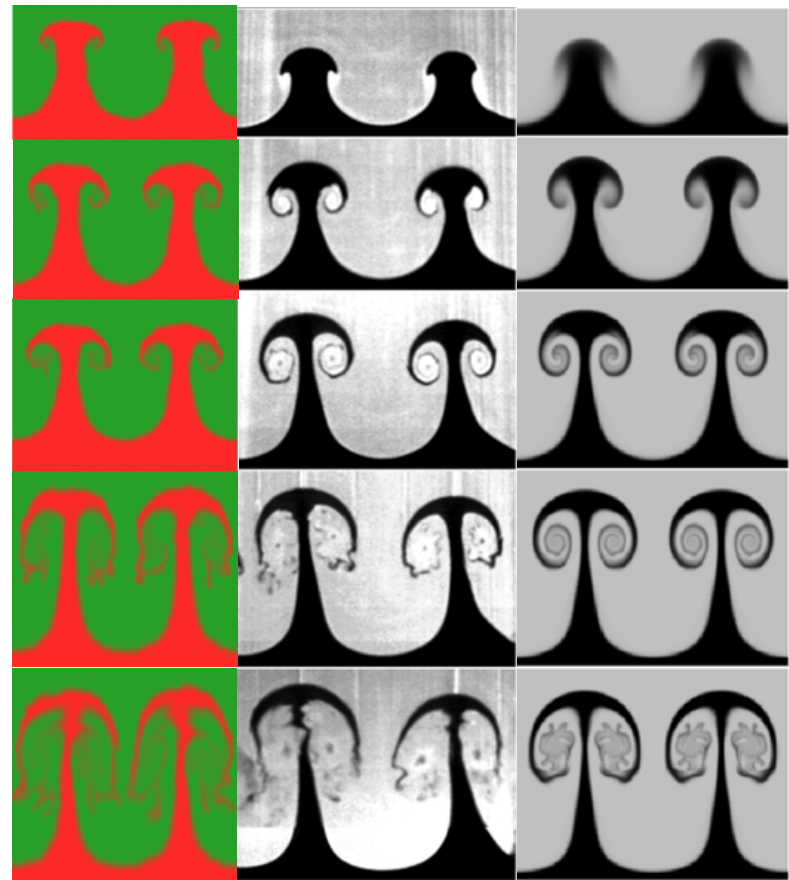
Interface moves with constant speed until the interface gets re-shocked
The development of bubbles and spikes can be tracked independently

"Direct simulation Monte Carlo investigation of the Richtmyer-Meshkov instability", M. A. Gallis, T. P. Koehler, J. R. Torczynski, and S. J. Plimpton, Physics of Fluids 27, 084105 (2015); doi: 10.1063/1.4928338

RMI in Air-SF₆ Mixture: Mach = 1.4 Shock

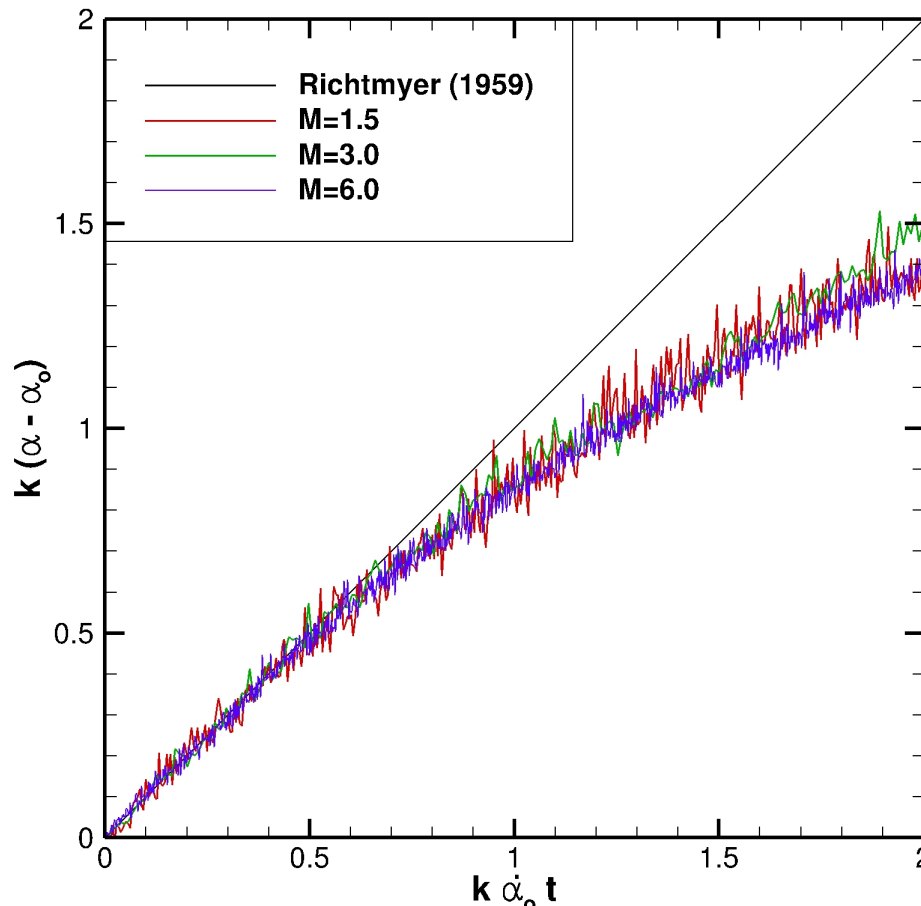


DSMC Experiment Navier-Stokes



Morgan *et al.* JFM 2012

RMI: Effect of Mach Number



Normalization indicates that Mach number plays a small role
 None of the theoretical models accounts for Mach number

Conclusions

DSMC yields exquisite agreement with analytical and experimental results, where available

DSMC scales extremely well & can take full advantage of massively parallel platforms

- Can simulate unprecedented flow regimes
- Hydrodynamic instabilities, lower altitudes

